Characterising the variability of the Indonesian Throughflow in ocean models

By Fan Zhang

Bachelor of Marine and Antarctic Science with Honours University of Tasmania, July 2019

A thesis submitted in partial fulfilment of the requirements of the Bachelor of Marine and Antarctic Science with Honours at the Institute for Marine and Antarctic studies (IMAS), University of Tasmania

June 2020

Declaration

This thesis contains no material which has been accepted for the award of any other degree or diploma in any tertiary institution, and that, to the best of the candidate's knowledge and belief, the thesis contains no material previously published or written by another person, except where due reference is made in the text of the thesis.

张帆
Fan Zhang

Fan Zhang

19 June 2020

Abstract

The Indonesian Throughflow (ITF) is the only ocean current that connects the Pacific Ocean and the Indian Ocean in the tropics. As such, the ITF plays an essential role in ocean circulation and regional climate: it hosts strong mixing that can change water-mass properties, influences the sea surface temperature in both oceans and affects the global ocean volume and heat transports. The ITF transports water properties across Indonesian Seas characterized by complex topography with most of the water entering through two main inflow straits, Makassar and Lifamatola straits, and exiting into the Indian Ocean through three main outflow straits, Ombai, Lombok and Timor straits. The ITF has been observed in major outflow straits and shows variabilities on different time scales, including decadal, interannual, seasonal and intra-seasonal. The ITF variability on intra-seasonal time scales is driven by remotely generated Kelvin and Rossby waves that propagate into the Indonesian Seas from the Indian Ocean and Pacific Ocean. In this project, we focus on the variability driven by Kelvin waves that propagate into Indonesian seas through three main outflow straits (Ombai, Lombok and Timor). We use a global ocean model and a high-resolution regional ITF model to characterize these variabilities at different depths and in different straits. We also use the mooring observations from the INSTANT program to validate the ocean models.

The simulation from the global model qualitatively agrees with that from the regional ITF model and both are consistent with observations from the INSTANT program. Evolution of a temperature anomaly associated with the eastward propagation of a Kelvin wave as it propagates towards Indonesian Seas is examined in two models. Our results suggest that the Ombai strait is the primary passage for Kelvin waves propagating into the Indonesian seas. Lombok strait accounts for some wave propagation northward into the Indonesia Seas and only a small number of Kelvin waves anomalies propagate through the Timor strait. Quantitatively, however, there are some differences between global and regional models as well as between the two models and observations. The amplitude of temperature anomaly in the regional ITF model is smaller than that in the global model. Also, the regional model does not capture the Kelvin waves well below 800m depth. Finally, the power frequency spectra corresponding to Kelvin waves is much bigger in observations than that in models at different depth consistent with low anomalies seen in models.

Acknowledgement

First, I would like to thank my supervisor, Maxim Nikurashin, who has rigorous academics, profound knowledge and broad vision, which has created a good academic atmosphere for me in the process of writing this thesis. Working with him, made me not only accept new ideas, set clear academic goals, grasp the basic way of thinking, master general research methods, but also understand many truths about how to treat people and deal with others. He has reviewed the full text many times in his busy schedule, amended the details, and provided many pertinent and valuable opinions for the writing of this article. I would also like to thank my senior student Yu Wang, who helped me a lot with the knowledge of programming and the skills of writing. What is more, I would like to thank for company and encouragement, my parents Handong Zhang and Qiuxia Tian, as well as my friends Hongkun Zhang, Li Chen, Kai Yang, Yaowen Zheng. Finally, I would like to thank the Ocean University of China (OUC) and the Institute for Marine and Antarctic Studies (IMAS) for providing me the opportunity to study physical oceanography and work on this research project.

Content

1. Introduction

1.1 Circulation of the Indonesian Throughflow

The ocean current that passes through the Indonesian seas from the Pacific Ocean to the Indian Ocean, known as the Indonesian Throughflow (ITF), is the unique pathway that connects these two ocean basins at low latitudes. There are 5 main large Indonesian seas: two shallow seas, the Arafura Sea and the Java Sea; and three deep seas, the Flores, the Banda and the Timor Seas (Sprintall et al., 2009a). Due to the complexity of topography in this region, the ITF is comprised of a myriad of narrow flows that permit the transfer of water between seas and basins of different size and depth level (Sprintall et al., 2019b), including several inflows and outflow passages.

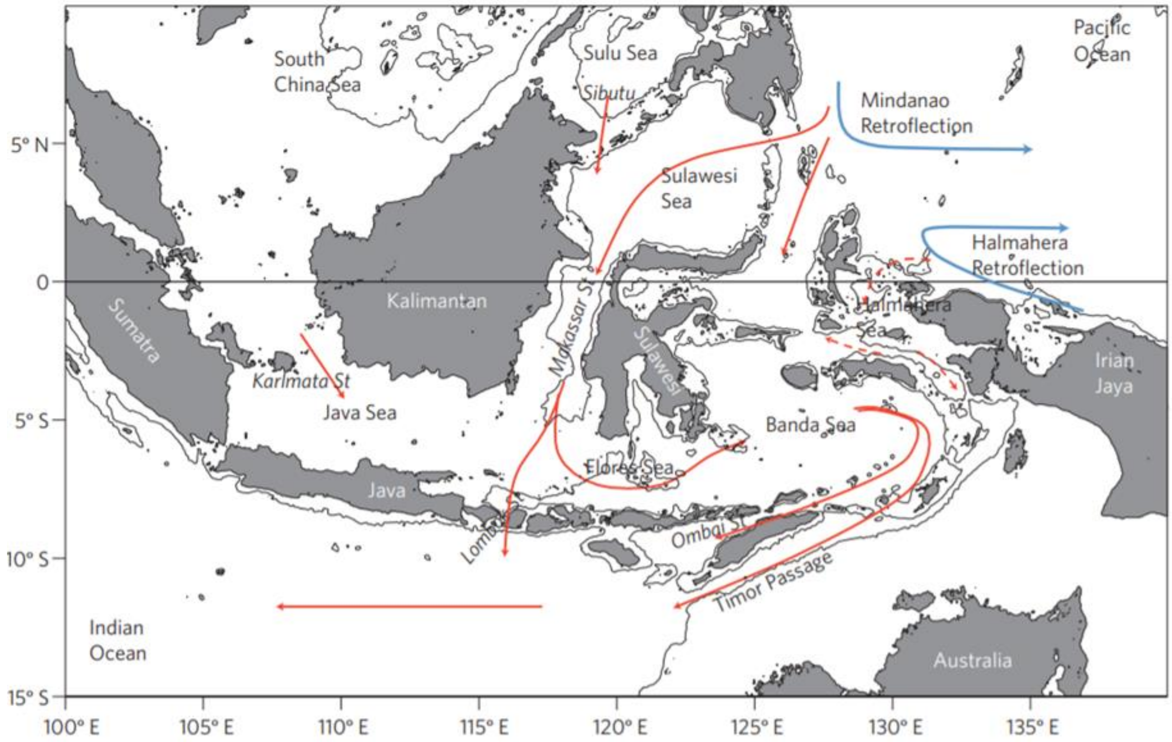

Figure 1 | Bathymetric and geographic features of the Indonesian seas (Sprintall et al., 2014a).

Red lines: The mean pathway of the Indonesian throughflow.

Dashed lines: Throughflow from the South Pacific.

The Makassar Strait is the primary inflow passage of the ITF which transports about 80% of the whole ITF (Susanto and Gordon, 2005). It transports primarily thermocline and intermediate waters from the North Pacific Ocean and only permits the waters above the thermocline to enter the Banda Sea via the Flores Sea (Ffield and Gordon, 1992). The Lifamatola Passage is the secondary ITF portal. It connects the deep layers of the Banda Sea, provides a source of freshwater via the Maluku Sea, and contributes water from the South Pacific Ocean through the Halmahera Sea. Smaller amounts of the ITF pass through the Karimata Strait (Fang et al., 2010) via the Sibutu Passage into the Sulawesi Sea (Gordon et al., 2012). Most of the ITF enters into the Indian Ocean through passages along the island chain in Nusa Tenggara via 3 main pathways: Lombok Strait, Ombai Strait, and Timor Passage. Small amounts of exchange also occur across the wide but shallow shelf of north-western Australia (Gordon et al., 1997). Other passages into the Indian Ocean along the Nusa Tenggara island chain are so shallow they make little contribution to the ITF mass transport (Godfrey, 1996).

1.2 The role of the ITF in global ocean circulation and climate

The ITF is a unique tropical branch of the global ocean thermohaline circulation. It is located in the climatological centre of the deep atmospheric convection related to the rising branch of the Walker Circulation (Gordon, 1986). Therefore, the ITF plays an essential role in regional climate and climate variability by carrying freshwater and heat (Song and Gordon, 2004). According to the experiment conducted by Lee et al. (2002), changes to the ITF are likely to alter the air-sea heat flux, heat content and wind which induce variability of the Indo-Pacific precipitation and monsoon for the Indian Ocean.

Mixing occurring along the path of the ITF modifies water masses and hence ocean heat transport. Specifically, strong tides, monsoonal wind-caused upwelling and large air-sea fluxes mix and modify the salinity and temperature stratified water within the Indonesian seas (Koch-Larrouy et al., 2007). The temperature and salinity profile evolution along the ITF described by Sprintall et al. (2014) suggests that the ITF becomes nearly isohaline as a result of mixing. It seems that the water masses are altered after exiting the Banda sea. Notably, the salinity maximum in mid-thermocline and the salinity minimum in the intermediate depth of the water masses are eroded in the Maluku, Seram and Flores seas.

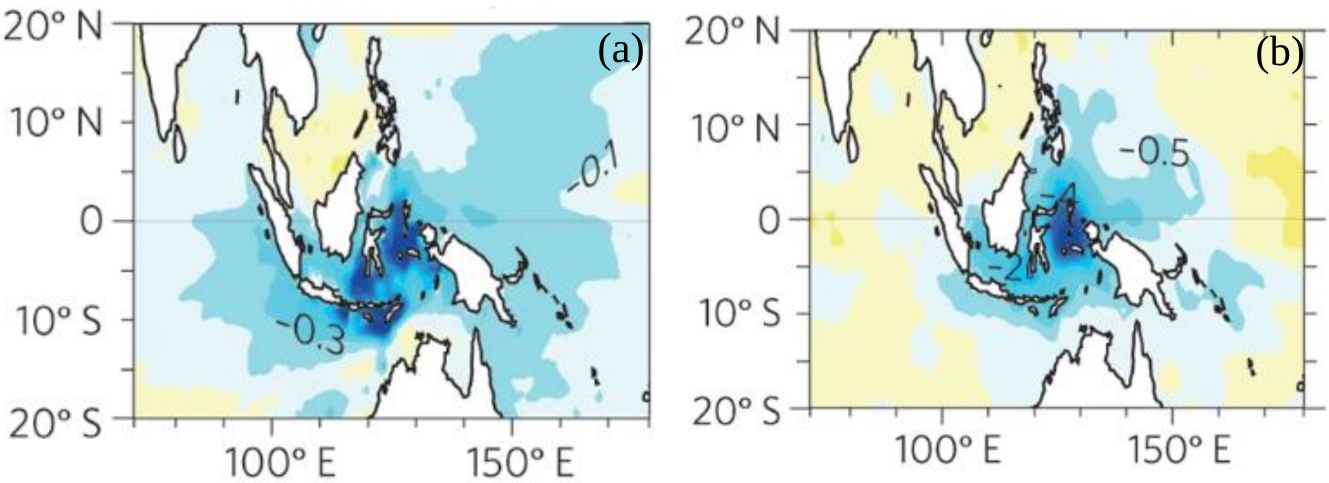

Figure 2 | Changes in ITF mean climate from models with and without tidal mixing parameterizations (Sprintall et al., 2014b).

(a): Differences in SST (°C)

(b). Differences in rainfall (mm)

Besides changing the water mass properties, the internal tide driven mixing within the Indonesian seas also makes a contribution to the sea surface temperature (SST) distribution which in turn modifies atmospheric convection, air-sea interaction and the monsoonal response (Kida and Wijffels, 2012). Sprintall et al. (2014b) used models to study the influence of the ITF for SST (Fig.2). Furthermore, coupled models developed by Koch-Larrouy et al. (2010) show that the SST of the Indonesian seas is cooled by the upwelling of the deeper waters driven by tidal mixing. To be specific, the temperature is dropped by about 0.5 °C and the ocean heat uptake increased by about 20 W m^{-2} in response to adding tidal mixing.

The volume transport through different passages of the ITF plays a crucial role in the ocean heat transport and hence the global overturning circulation. The heat transport via Indonesian seas is known to be warm and surface intensified with the transport weighted temperature between 22 to 24°C (Wyrtki, K, 1961), but with a mean temperature of about 13°C because of the subsurface maximum of the heat transport in Makassar Strait (Vranes et al., 2002). During the rainy northwest monsoon season, this cooling is active, especially when the water enters the Makassar Strait through the South China sea (Gordon et al., 2003). The cooling inflow via Makassar Strait largely moderates the warmer water from the outflow passage (Wijffels et al., 2008).

1.3 Variability of the ITF

Originally, the ITF was mainly thought to show distinct intra-seasonal variability driven by the regional southeast and northwest monsoon (Wyrtki, K, 1961). However the comprehensive research of Gordon et al. (2008) revealed that the ITF shows strong variability on different time scales including decadal, interannual, seasonal and intra-seasonal variability.

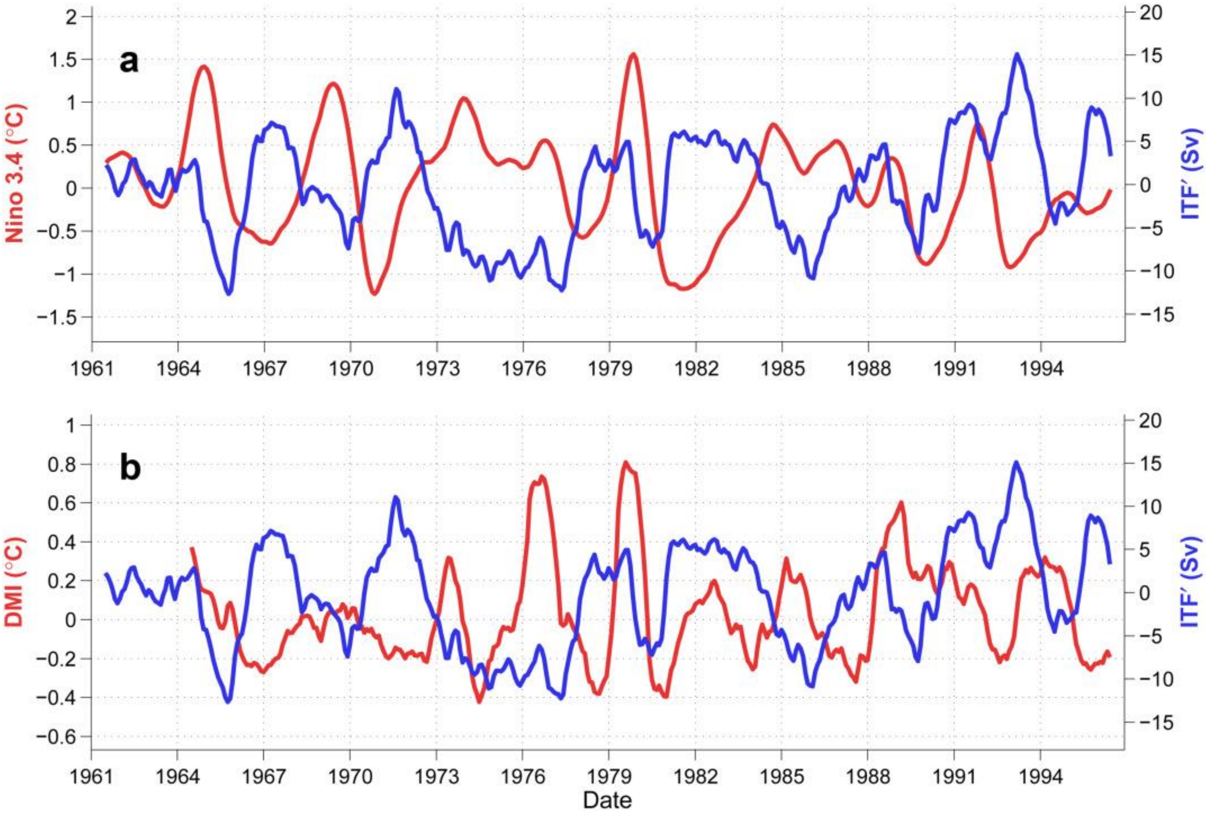

Figure 3 | Comparison between ensemble mean of ITF transport anomaly (blue) and the (a) Niño 3.4 index (red) and (b) DMI index (red) on decadal time scale (Hu and Sprintall, 2016).

For the *decadal* timescales, the circulation of the Indonesian seas is altered by the trade wind system in the Pacific Ocean. Hu and Sprintall (2016) explored the mean of the ITF transport anomaly from 1961 to 2000 (Fig.3). In the 1970s, a part of the Walker Circulation became weaker and caused anomalies of the shallow thermocline in western Pacific (Vecchi et al., 2006). When the ITF exited into the Indian Ocean, Wainwright et al. (2008) observed that there was a warmer surface, cooler subsurface and a net reduction in volume transport. Many models suggested that there was a relationship between this trend, carried by the ITF, and the lessening of the trade wind in the Pacific Ocean (Alory et al., 2007). From the 1990s to now, there has been a constantly strengthening east wind in the Pacific which leads to cooling for the Indian Ocean and subsequently raises the sea level of the western Pacific Ocean in low-latitudes (Schwarzkopf and Böning, 2011).

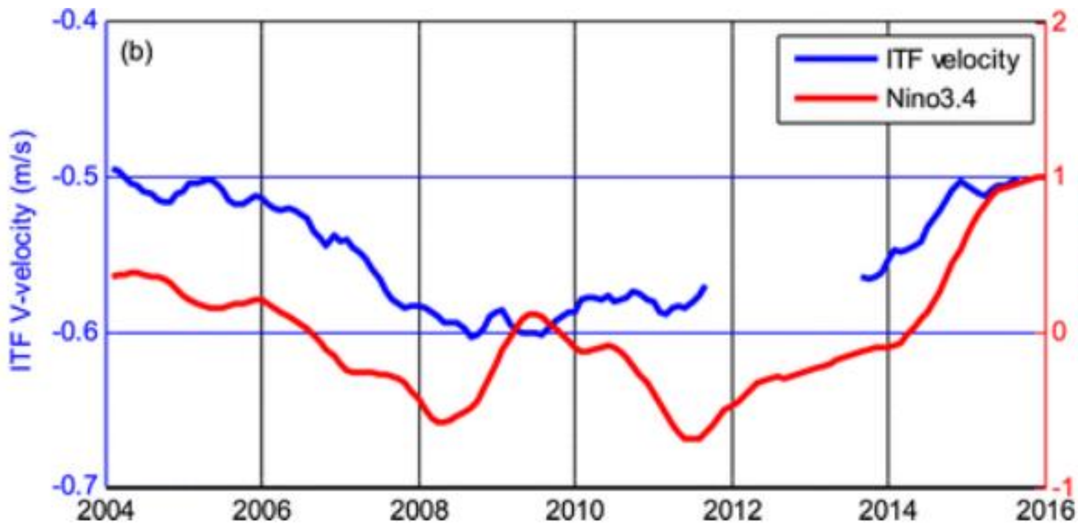

Figure 4 | 12-month running means of the ITF *υ* velocity and Niño-3.4 index (Wei et al., 2016).

Interannual variability is also significant. The ITF in the Makassar Strait becomes shallower and continually stronger according to the observation of Gordon et al. (2012). The maximum speed of thermocline has risen from 70 to 90 cm s^{-1}, and the depth has reduced by nearly half since 2007. As a result, there is a 47% enhancement in transport between 50 and 150 m depth (Sprintall et al., 2014a). From the 1990s to the mid-2000s, more frequent and intense El Niño and La Niña conditions have caused a massive variation in the transport profile of the ITF. The surface throughflow in the Makassar Strait is reduced during El Niño episodes, and the upper layer of the thermocline is shoaled and strengthened during the period of La Niña (Sprintall and Révelard, 2014). The surface heat fluxes and stratification of the Indian Ocean can also be regulated by La Niña events that warm the SST in Indonesian seas (Song and Gordon, 2004).

(a)

(b)

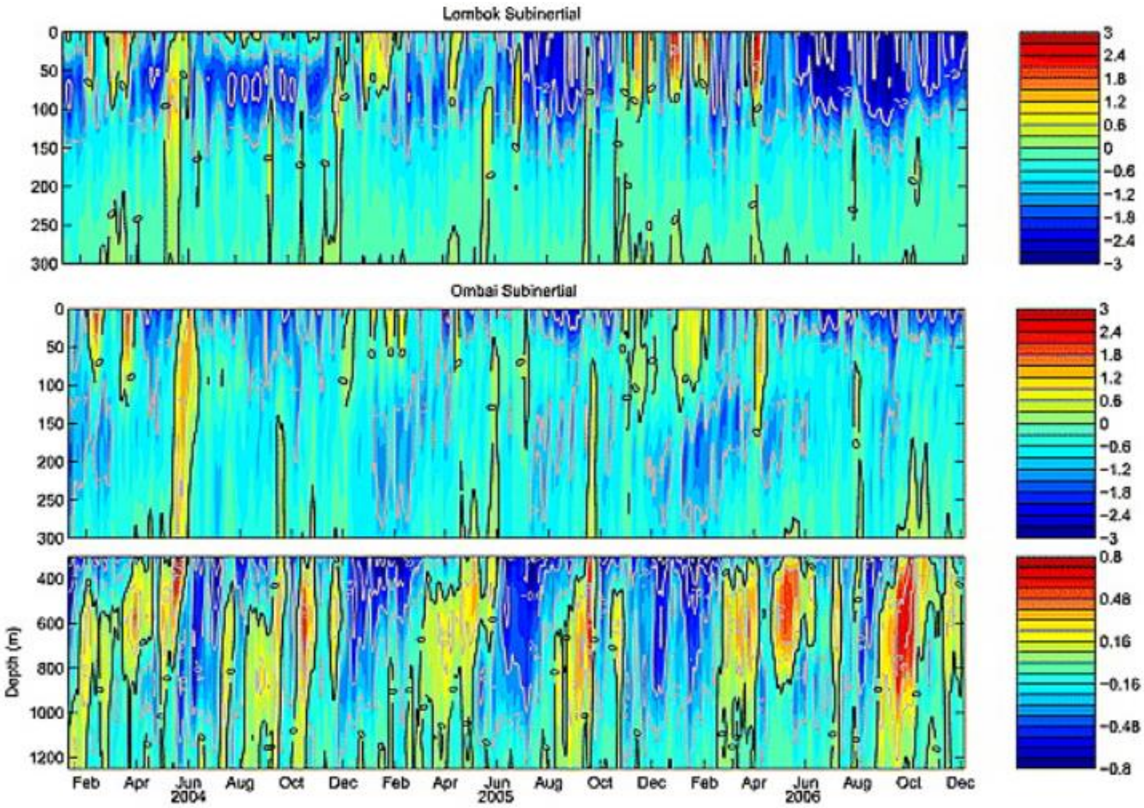

Figure 5 | Vertical distribution of subinertial transport per unit depth (10^{-2} Sv m^{-1}) for (a) Lombok Strait, (b) Ombai Strait on seasonal and intra-seasonal time scales from 2004 to 2006 (Sprintall et al., 2009b).

The ITF also shows a prominent *seasonal* variability. For instance, Fig.5 shows the variability of the ITF from 2004 to 2006 including both seasonal and intra-seasonal variabilities. Wyrtki (1961) showed that there is a complicated and substantial variability in the circulation within the Indonesian seas which is caused by the monsoon winds from Asia and Australia. Masumoto and Yamagata (1996) used an Indo-Pacific Ocean General Circulation Model (OCGM), which permits the barotropic Indonesian throughflow, to investigate the seasonal transport variability of the ITF in the Indonesian areas. According to the model, the annual mean transport through the Indonesian Seas is 9.5Sv. There is a maximum transport of 11.6Sv in August and a minimum transport of 6.0Sv in January. The regional monsoon winds, and the variation of sea level which is activated remotely in the eastern and central area of the Indian Ocean near the equator, are thought to impact the seasonal transport variability via the Lombok Strait. The seasonal variability of inter-basin throughflow is modulated by these variations in the eastern Indian Ocean and Indonesian Seas (Masumoto and Yamagata, 1993).

In addition, there is significant *intra-seasonal* variability of the ITF. A variety of locations around the Indonesian Seas have observed oscillations on the intra-seasonal time scale in sea surface temperature and sea level. The dynamics of intra-seasonal variability in the ITF has been investigated by many research teams using different models. For example, a semi-annual Indian Ocean forced Kelvin wave was observed in the Indonesian seas in May 1997 by Sprintall et al. (2000). The semi-annual variability linked to Kelvin waves will be discussed in detail in the next section. Iskandar et al. (2006) used a high-resolution OGCM to reveal that a 90-day variation dominates the South Java Coastal Current (SJCC), which is the surface current in the Indonesian Seas. The subsurface current, the South Java Coastal Undercurrent (SJCU), mainly features 60-day variations. Qiu et al. (1999) used a fine-resolution 1½-layer reduced-gravity model to show that the throughflow in the Makassar Strait and the Banda Sea is influenced by a 50-day oscillation of the Celebes Sea. However, the variations of throughflow from Lombok, Ombai, and the Timor Straits are not impacted by the oscillation significantly.

1.4 Intra-seasonal variability and its drivers

The intra-seasonal variability of the ITF has attracted much attention which is associated with the circulation and climate in the Indonesian seas (Sprintall et al., 2019b). The dominant intra-seasonal variability is believed to be driven by remotely generated waves propagating into the Indonesian Seas. The Rossby and Kelvin waves generated by the zonal winds from the Indian and the Pacific Ocean near the equator are thought to cause the variability of the temperature and sea level of the ITF on the intra-seasonal time scale (Wijffels and Meyers, 2004).

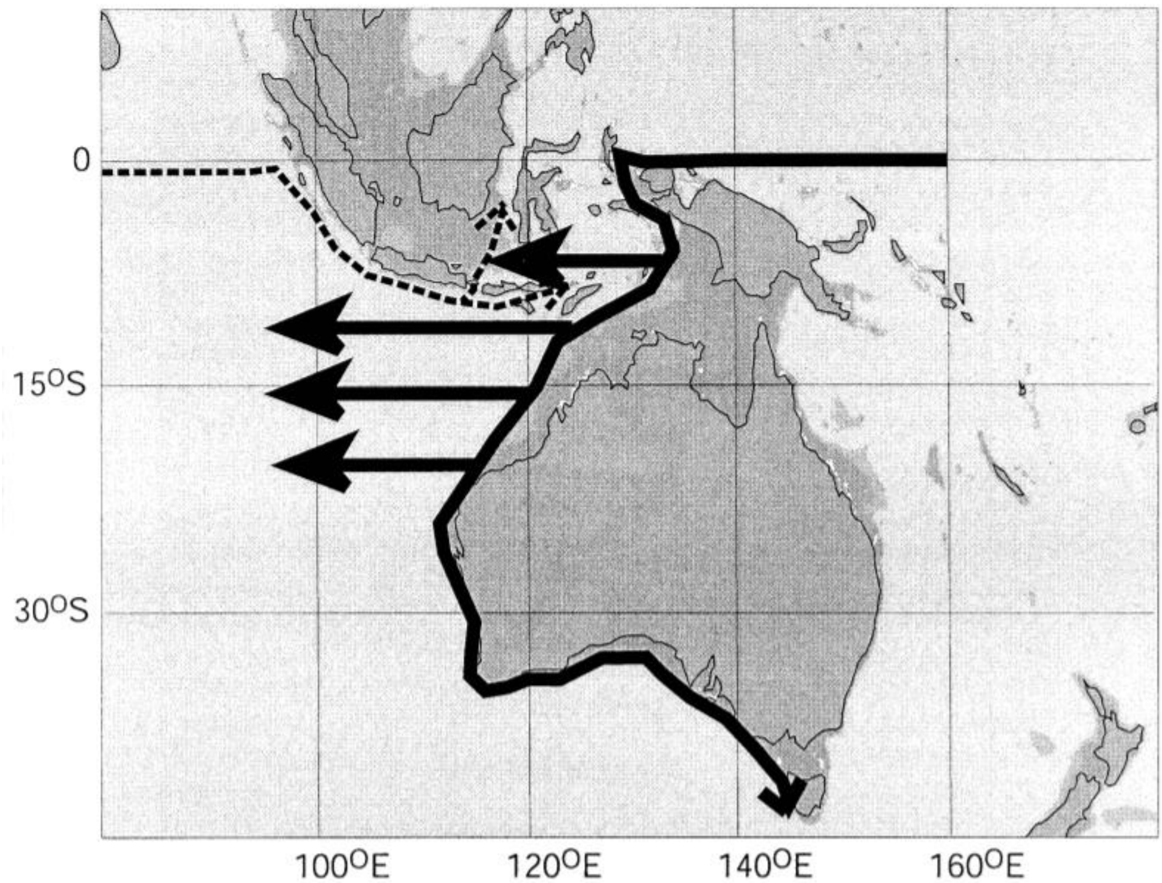

Figure 6 | Pathways of the remotely forced wave into the throughflow region (Wijffels and Meyers, 2004).

Thin broken lines: Eastward propagating Kelvin waves

Solid black arrows (leftward): Westward propagating Rossby waves

The Kelvin waves: The generation mechanism of Kelvin waves is described by Wyrtki (1973): During the period of monsoon transition from April to May, and October to November, there is a Yoshida-Wyrtki Jet that occurs twice a year in the Equatorial Indian Ocean. The jet mainly concentrates on the Equator and extends eastward. When it reaches the eastern boundary, it continues to propagate poleward along the coast of the Indonesian seas and then becomes coastal Kelvin waves. Therefore, the Kelvin wave in Indonesian seas occurs semiannually: there is a downwelling Kelvin wave which is caused by the negative anomaly and an upwelling Kelvin wave that is caused by the negative anomaly each year. The pathways of the remotely forced wave into the throughflow region are shown in Fig.6 (Wijffels and Meyers, 2004).

A semiannual Kelvin wave was observed by Sprintall et al. (2000). The wave is generated at the equator in the Indian Ocean and then goes southeastward along the coast of Sumatra or Java via the Lombok Strait, as well as northward to the Makassar Strait. Also, by the observation of a mooring located there, some currents were observed to reverse. A simple wind-forced Kelvin wave model is thought to account for the variability of sea level from Nusa Tenggara to the Ombai Strait, which indicates the Indian Ocean winds drive the variability remotely in these areas. In the same way, Hautala et al. (2001) suggested that downward Kelvin waves near the equator could account for the shallow coastal South Java Current that flows eastward to the Ombai Strait. According to their study, the variability changes with location. For instance, the variability in the Timor Strait had less similarity with that in the straits farther west and north, which implied the east coast of Timor cannot be reached by the wind energy from the Indian Ocean. In both the Ombai and Timor Straits, a large amount of intra-seasonal energy was found (Molcard et al., 1996). Throughflow reversals in the Ombai Strait driven by Kelvin waves, which are forced in the Indian Ocean, were observed by Sprintall et al. (2000) and Potemra (2001).

The Rossby waves: Similar to the generation of Kelvin waves in the Indian Ocean, low-frequency wind energy is driven remotely from the Pacific Ocean into the Indonesian Seas by Rossby waves. This energy can go through into the throughflow region and then flow southward along the western coast of Australia, which modulates the thermocline and sea level. So it is almost consistent with the El Niño–Southern Oscillation (ENSO) (Pariwono et al., 1986). The anomalies of zonal wind in the Pacific Ocean near the central equator generate the equatorial Rossby waves, and there are coastal-trapped waves in the coast of New Guinea which intersect the equator. It is the transmission of the Rossby waves to the coastally trapped waves that is thought to increase remote energy. The coastally trapped waves will spread around not only the western edge of New Guinea but also poleward along the continental margin of Western Australia. Some of the wind-driven wave energy from the Pacific is observed as free Rossby Waves which propagate westward through the Banda Sea and into the southern Indian Ocean in tropical ocean. The regional response to the strong forcing by monsoon winds is intensified within several months (Meyers, 1996). Furthermore, Potemra (2001) used a 1½-layer model to show there was a leak of energy from the Pacific Ocean into the Indian Ocean on a semiannual time scale.

This thesis will focus on Kelvin waves primarily because they arrive in the Lombok, Ombai and Timor passages from the Indian Ocean and are well captured by mooring observations in those passages. The observations are used here to validate ocean model results. Similar intra-seasonal variability is driven by Rossby waves in the north of Indonesian Seas, but it will not be discussed in this thesis.

1.5 Summary

The ITF plays an essential role in global ocean circulation and the climate system and shows variability on different time scales. This is driven by remotely generated Rossby and Kelvin waves which propagate into the Indonesian seas from the Pacific and Indian Oceans. Kelvin and Rossby waves may also play an important role in circulation for the local Indonesian Seas through energy radiation into this region, leading to energy dissipation and mixing. The characteristics of Kelvin and Rossby waves in an ocean model may depend on the model resolution, bathymetry representation, and parameterization of subgrid-scale processes in the model, as well as the model forcing. How well ocean models reproduce those remotely generated waves and hence the intra-seasonal variability of the ITF has not been assessed before. This study will focus on the evaluation of intra-seasonal variability in ocean models which is the first step towards understanding the energetics of intra-seasonal wave-driven variability and its impact on the ITF circulation and climate.

2. Methods

To characterize the variability and validate ocean models, we used available mooring observations from the INSTANT program and compared them to simulations from a global ocean model widely used in Australia, and a regional ocean model recently developed for process studies in this region.

2.1 INSTANT data

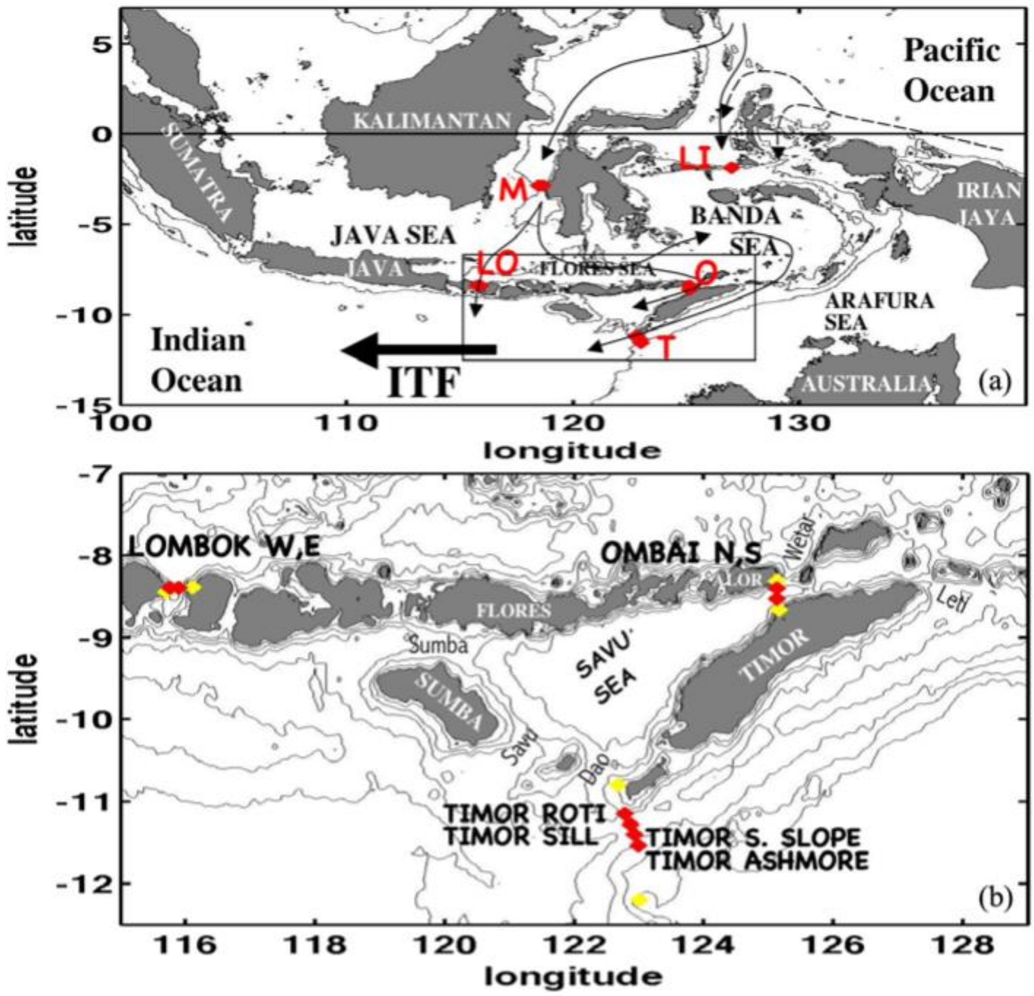

Figure 7 | The location of mooring (Sprintall et al., 2009b).

(a) The location of INSTANT moorings deployed in two inflow passages: Makassar Strait (M) and Lifamatola Strait (LI), and three outflow passages: Lombok Strait (LO), Ombai Strait (O), and Timor Passage (T)

(b) Red diamonds: the location of INSTANT mooring

(c) Yellow diamonds: shallow pressure gauges in the exit passages along Nusa Tenggara.

We used observations of the multiyear variability of the ITF from the International Nusantara Stratification and Transport (INSTANT) program which deployed an array of 11 moorings to measure the ITF (Sprintall et al., 2004). The full depth in situ velocity, salinity and temperature profiles of the ITF were measured by the mooring array for more than 3 years. The moorings were located in the two main inflow pathways of the Makassar and Lifamatola Straits and the three main outflow pathways of the Lombok, Ombai and Timor Straits

(Sprintall et al., 2009b). (The observations were made available to this project for the model validation through the supervisor and collaborators at CSIRO.)

Ombai Strait is 37 km wide, and there were two moorings (Ombai North and Ombai South) at -3250m depth. Lombok Strait is 35 km wide, and there were two moorings at the east and west of the strait, which were deployed at 300m sill. The current around the sill is so strong that a tall mooring cannot be deployed, hence, the mooring was positioned at the north of the sill. Four moorings (Timor Roti, Timor Sill, Timor South Slope, and Timor Ashmore) were deployed at the Timor passage, which is 160km wide. At the eastern edge, the moorings were deployed at 1250m, while the moorings at western Timor were deployed at 1890m. The velocity instrumentation configuration of all moorings was fairly similar. An upward-looking Acoustic Doppler Current Profiler (ADCP) was deployed at each mooring in order to resolve the flow from surface to thermocline. To resolve the sub-thermocline to intermediate depth flow, the single-point current meters were positioned at depth.

To validate model simulations in this project, we used velocity and temperature time series from the Ombai south mooring in Ombai strait. The spectrum frequency calculated according to the velocity in this mooring will be used as well.

2.2 Models

In this project, we used three models to simulate the ITF and its variability: two models were global ocean models at 0.1-degree resolution (used in Australia for ocean simulations), and one model was a process-study regional model used to study processes within the ITF region at a range of resolutions. These three models have different configurations, including resolution and subgrid-scale physics representation, and are driven by different forcing. Therefore, they can give different representations of the intra-seasonal variability. The regional model is forced by open boundary and surface forcing from one of the global models through a one-way nesting approach. Hence, the results from only one global model and a regional model are shown and discussed in the Results section below, while configurations of all three models are described in the Methods section.

2.21 OFAM3

OFAM3 is a shortened form of the Ocean Forecasting Australian Model, version 3. It is a global model which can provide the forecast for the circulation in mesoscale at low and mid-latitudes. OFAM3 is based on a Modular Ocean Model with a z^* configuration of version 4p1, which is nearly global and can resolve eddies (Griffies, 2009). The aim of this model is to hindcast and forecast the condition of the upper ocean in tropical and temperate zones. From 75^{o}N to 75^{o}S, there is a 1/10^o grid spacing of total longitudes for the model grid. The vertical resolution is 5m at 40m depth, while the resolution is 10m at 200m depth (Oke et al., 2013).

The forcing is freshwater, surface heat and momentum fluxes based on ERA-Interim (Dee and Uppala, 2009). The surface temperature is restored to observations that are monthly averaged, and the timescale of restoring is 10 days. Similarly, surface salinity is restored to climatology that is monthly averaged, but the timescale is 30 days. This model is forced by a fully realistic forcing that has variability ranging from high-frequency daily to interannual.

The 30-arcsecond GEBCO_08 topography and 9-arcsecond topography produced by Geoscience Australia derive the topography of OFAM3 (Whiteway, 2009). The model has a minimum depth of 15m. The real topography which is less than 15m in some regions is set to zero or 15m in the model.

2.22 ACCESS-OM2-01

This model has similar resolution to OFAM3 but also includes sea ice and is run with two different types of forcing: (1) repeat year forcing and (2) inter-annual forcing. There are also differences in model configurations between OFAM3 and ACCESS-OM2-01. ACCESS-OM2-01 is a more recent model, likely to be used in Australia for model simulations in the future. Outputs from ACCESS-OM2-01 are used as open boundary conditions to drive the regional, process-study model of the ITF described below.

The ocean-sea ice component of the Australian Community Climate and Earth System Simulation is known as ACCESS-OM2. It is a global model designed to support the development of climate models and forecasts of the ocean state in Australia. The ocean model component is the Modular Ocean Model (MOM) version 5.1 that is from the Geophysical Fluid Dynamics Laboratory (Kiss et al., 2019). The sea ice model component is a branch of the Los Alamos sea ice model (CICE) version 5.1.2 from Los Alamos National Laboratories.

There are three horizontal resolutions available: The 1◦ horizontal grid spacing named ACCESS-OM2, 0.25◦ spacing named ACCESS-OM2-025 and 0.1◦ spacing named ACCESS-OM2-01 (Kiss et al., 2019). The latter 0.1-degree resolution model was used in this project. The vertical grid spacing in ACCESS-OM2-01 is 1.1m with 75 levels. In order to facilitate the research of sub-grid scale parameterization and resolution dependence, the configurations (such as forcing and run parameters) are made to be consistent across the different resolutions (Kiss et al., 2019).

The JRA55-do v1.3 atmospheric product provides the atmospheric forcing for the model: downward shortwave and longwave radiation fluxes; rainfall, snowfall and runoff fluxes; surface pressure; 10m air temperature and specific humidity; and 10 m wind vector (Tsujino et al., 2018). Partial cells are used to represent the bottom topography. The minimum water depth is 10.43m with 7 levels in ACCESS-OM2-01 (Adcroft et al., 1997).

2.23 High-resolution regional model

This model is forced by repeat-year forcing and open boundary fields from ACCESS-OM2-01, but has simulations at a range of resolutions: 10km, 4km, and 1km. In this project, we analyzed the 10km resolution model as a first step to validate the model performance. This resolution is similar to the resolution of the OFAM3 model and should be sufficiently high to resolve the incoming Kelvin waves from the Indian Ocean. The interaction of these waves with the complex topography of the Indonesian seas may be better represented by higher resolution models. The impact of resolution on wave simulation and intra-seasonal variability is planned to be addressed in future studies.

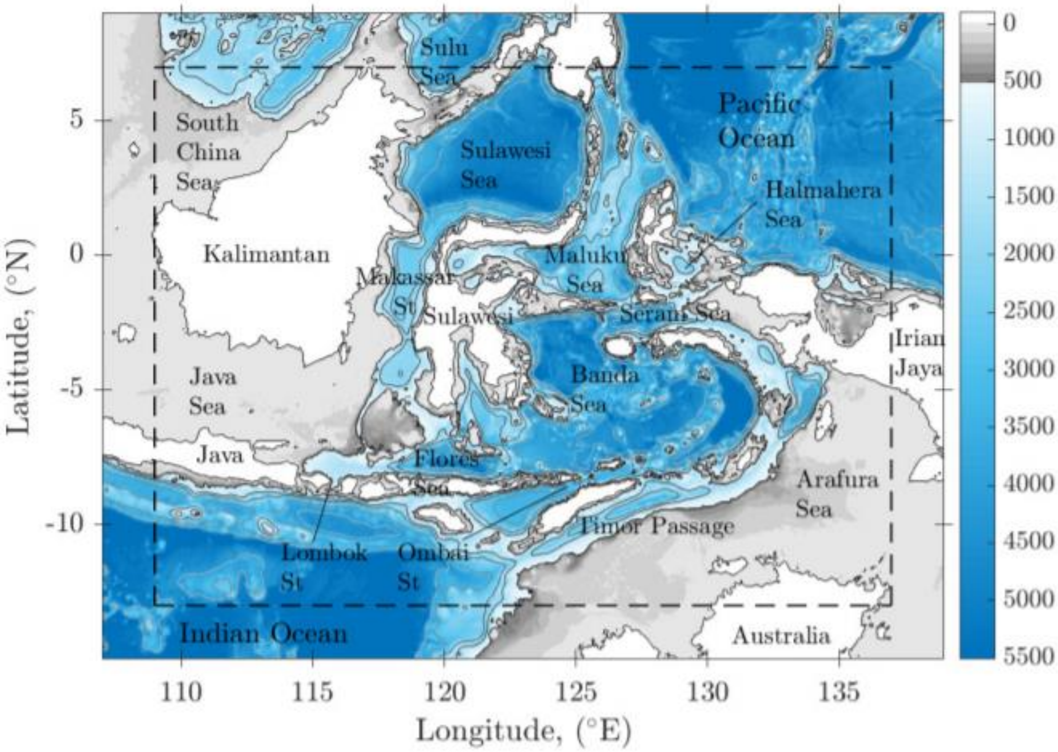

Figure 8 | Map of the domain. The black dashed lines correspond to the maximum extension of the lateral sponge layers (O. Richet, 2019).

The high-resolution regional model of the ITF is based on the Massachusetts Institute of Technology general circulation model (MITgcm) (Marshall et al., 1997). MITgcm has been used to study Indonesian Seas before, in studies of the influence of internal tides on the ocean ecosystem (Kelly et al., 2015) for instance.

The model used in this study was developed by my supervisor, Maxim Nikurashin, and collaborators (Richet et al. 2019). It has a three-dimensional domain that is on the spherical polar grid as well as an open lateral boundary. There is a 2^{o} thick sponge layer at each lateral boundary. Toward the boundary the salinity, meridional and zonal velocity, and temperature are restored to fields obtained from the ACCESS-OM2-01 global ocean model. There are 100 verticals levels in the domain with a 5.5km total depth. The vertical resolution is 2.1m at the surface which increases exponentially to 263 m to the deepest grid cell (O. Richet, 2019).

The ACCESS-OM2-01 model provides the forcing, such as salinity and temperature, on open boundary and surface conditions as well as the surface wind stress (Tsujino et al., 2018). The domain has a free surface. The high-resolution bathymetry SRTM30 PLUS was used in this model. At the bottom boundary, the quadratic drag and no-slip condition was adopted. The model was run in hydrostatic configuration, and the non-local K-Profile Parametrization (KPP) scheme was applied for subgrid-scale processes related to vertical mixing (O. Richet, 2019)).

3. Results

In this section, we present the analysis of the ITF variability in the observations from INSTANT and simulations from models with an emphasis on intra-seasonal Kelvin wave driven variability. First, we will present the results from the INSTANT program and then we will analyze the models and compare them to observations.

3.1 Variability from the INSTANT program

The INSTANT program provides mooring observations of the ITF that have been extensively studied and described in the literature previously. (For instance, Sprintall et al. (2009b) studied the mean transport of the Indonesian Throughflow (ITF) and its variability by analyzing the full-depth velocity measurements from the INSTANT program.) In this project, we characterized the variability of the ITF and its representation in ocean models and hence we validated these models with observations as part of this project. The observations from INSTANT were a perfect choice for this validation as they capture variability in three outflow straits into the Indian Ocean, in which the flow is affected by the eastward propagating Kelvin waves. In our model analysis below, we mainly focus on the temperature and velocity anomalies as diagnostics to show the intra-seasonal variability generated by Kelvin waves. Hence, in this section, we first give examples of some diagnostics from the INSTANT program that the model results will then be compared to. As an example, we present the time series of temperature and velocity anomalies versus depth in the Ombai Strait and the corresponding kinetic energy spectra at different depths. We will use this example to discuss and characterize the seasonal and intra-seasonal variabilities and indicate the presence of Kelvin waves in one of the major outflow straits into the Indian Ocean. Then, these diagnostics for all three straits (Ombai, Lombok and Timor) will be used as a reference to compare to the results from the models.

3.11 Temperature and velocity time series

The temperature and velocity variability in the Ombai Strait (from INSTANT) is shown in Fig. 9a and 9b, respectively**.** These two figures show the temperature and along strait velocity anomalies versus depth from 2004 to 2006. Although the data from about 200m to 0m depth in Fig.9a was not recorded for the whole duration of the program, the seasonal cycle of the ITF can clearly be seen in the upper ocean. The seasonal cycle is more evident in temperature than in velocity. The data from Jan to Dec 2006 show strong seasonal variability with an amplitude of up to ± 2 ^{0}C corresponding to the change of the seasonal monsoon. The temperature anomaly is positive during Dec to Jun and negative for the rest of the year. Below the 200m depth, there are strong temperature signals which are more frequent and have smaller amplitude than those corresponding to seasonal variability in the upper ocean. The amplitude of those signals is about ± 1 ^{0}C. These signals are regarded as the intra-seasonal variability because of their shorter duration. In April and May 2006, from the 300m to 600m depth in the Ombai Strait, the strong negative temperature anomaly is the clear signature that shows an upwelling Kelvin wave generated in response to wind reversals in the equatorial Indian Ocean during the Monsoon Transition Season (MTS). Meanwhile, there is a positive temperature anomaly in Dec and Jan at a similar depth. The propagation of these Kelvin waves is consistent with the theory of equatorial Kelvin wave dynamics in the ocean (P.H. Leblond, 1978). Their duration is about 30-60 days and frequency are twice per year.

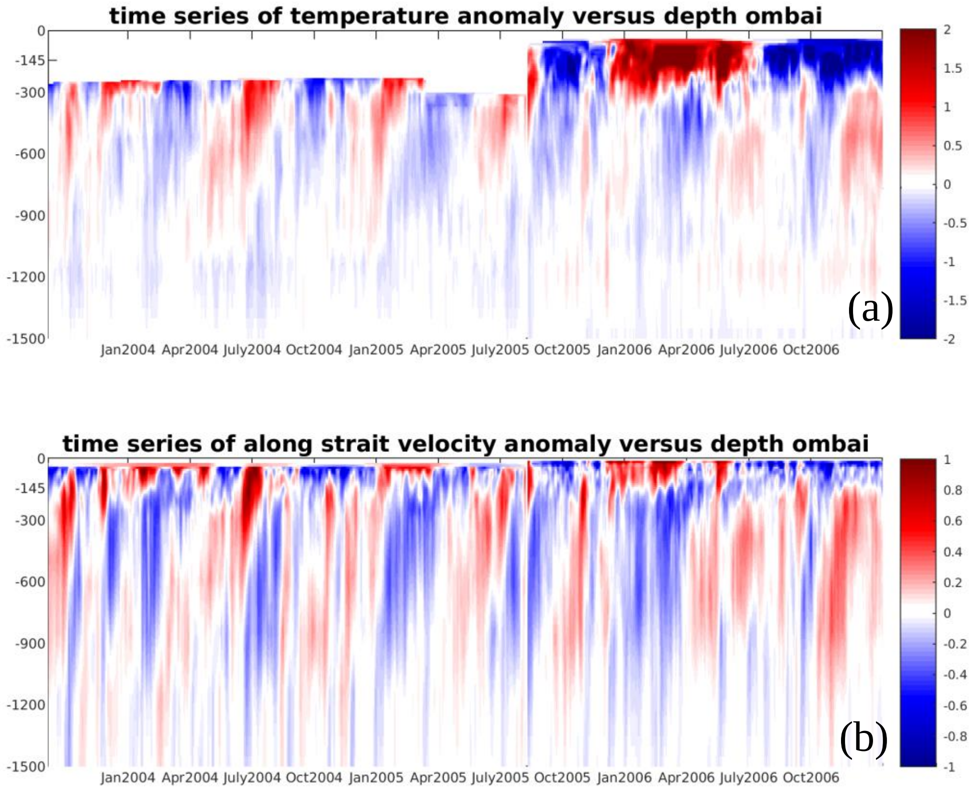

Figure 9 | (a) Time series of temperature anomalies versus depth (m) t moorings Ombai from INSTANT. Blue (red) denotes positive (negative) anomalies. Units are 0C. (10) Time series of velocity anomalies versus depth (m) at moorings Ombai from INSTANT. Blue (red) denotes positive (negative) anomalies. Units are m/s.

The observation of the along strait velocity anomaly is much more complete. Although some data at the surface from 2004 to 2005 is missing, Fig.9b shows clear regular seasonal variability in the upper layer over the period of 3 years. The velocity anomaly becomes positive from Dec to May and negative from June to Nov each year. Compared to the time series of temperature anomaly, the seasonal velocity variability seems to concentrate mainly in a shallower depth layer from 150m to the surface. The intra-seasonal variability begins to dominate at depths of around 150m. However, in addition to the semiannual variability representing Kelvin waves, other more frequent variability is also clearly seen. The velocity anomaly reaches its maximum of nearly ± 1 m/s at the surface, while it reduces to about ± 0.5 m/s for the intra-seasonal variability at depth.

In summary, the temperature and velocity anomaly time series from INSTANT show variability at different time scales and depths. The strongest variability is the seasonal cycle close to the surface. The intra-seasonal variability driven by Kelvin waves, the focus of this project, is also evident in the INSTANT observations.

3.12 Kinetic energy spectra

To provide a more quantitative analysis of the ITF variability at different frequencies and specifically to quantify the intra-seasonal variability at semi-annual, Kelvin-wave driven frequency, we now describe the kinetic energy spectra computed using velocity measurements from the INSTANT program. Fig.10 shows the time series of along strait velocity and the frequency spectrum at three depth levels. Because both the seasonal and intra-seasonal variability changes with depth, we choose 3 different depth levels: 140m, 300m, 500m. Seasonal variability in the ITF usually appears near the thermocline at about 100-150m depth to the surface (Sprintall et al., 2009b). So, any intra-seasonal variability signal in the upper ocean is superimposed with the seasonal variability signal. Hence, we choose 140m, which is roughly below the thermocline, as the first depth level. This depth also corresponds to the depth where the intra-seasonal variability begins to appear in the velocity anomaly depth-time series (Fig.9a). From Fig.9a and 9b, there are also plenty of strong and clear intra-seasonal variabilities in the deeper ocean above 600m depth. Hence, we also choose 300m and 500m to describe the intra-seasonal variability in the deeper ocean.

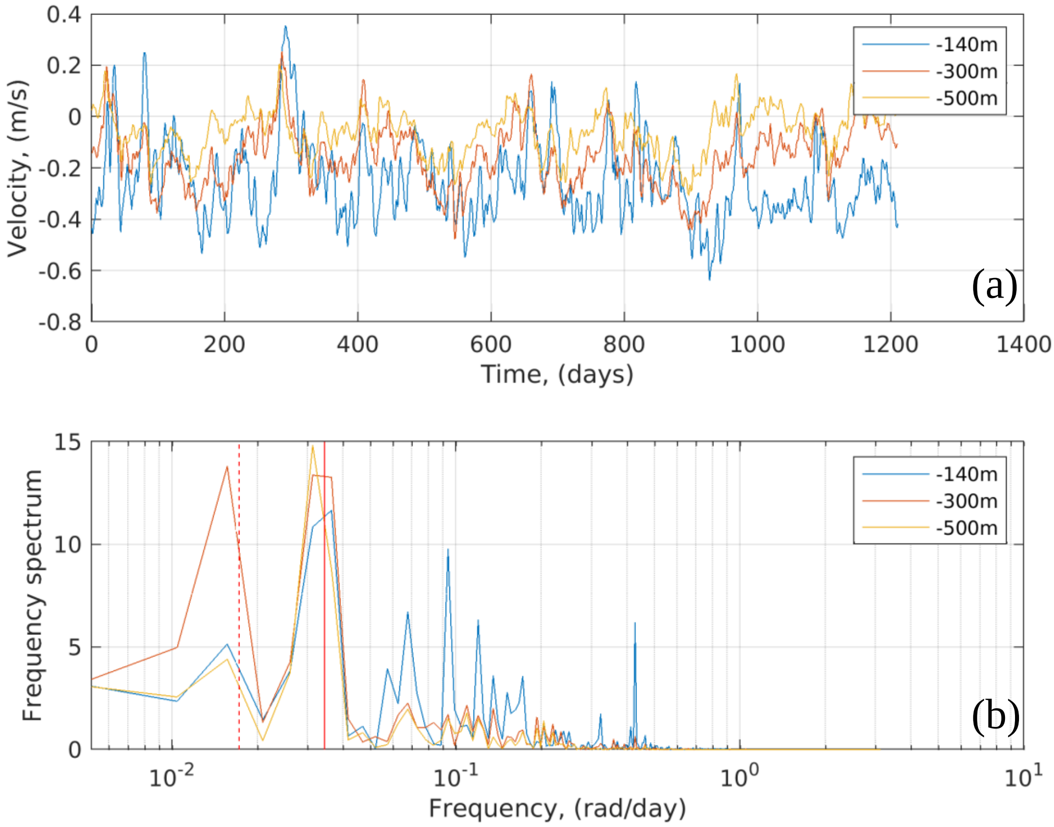

Figure 10 | Time series of along strait velocity (m/s) and frequency spectrum (m^2*day/s^2) in Ombai Strait at -140m, -300m and -500m depths.
Red dash line: The frequency which represents the period of one year.
Red line: The frequency which represents the period of a half year.

Fig. 10a shows the change of the along strait velocity with time at different depths in the Ombai Strait. The speed is negative most of the time indicating that the ITF mainly flows from Indonesian seas into the Indian ocean. The frequency spectra are calculated by the total velocity, which includes both the along strait component and across strait component. Fig. 10b clearly shows several peaks in the kinetic energy spectra corresponding to particular frequencies. The first peak has a period of one year and corresponds to the seasonal cycle. The second peak has a period of 180 days and corresponds to a semiannual Kelvin wave. The intra-seasonal variability is generally as strong as the seasonal one and at some depths even dominates.

Seasonal variability is thought to be strongest at the surface. According to the time series of temperature versus depth, the seasonal cycle concentrates in the upper layer. Therefore, we could expect that the seasonal variability should become weaker with depth. However, the seasonal variability indicated by the kinetic energy spectra estimated from velocity, shows that it is strongest at 300m depth. This is likely because the seasonal variability in the velocity signal is dominated by the variability of the flow, rather than by the local surface fluxes, which may dominate the temperature variability. Sprintall et al. (2009b) noted that the main core of the ITF is the subsurface during the northwest monsoon. Thus, the seasonal velocity variability is expected to be strong where the flow is strong. In contrast, the intra-seasonal variability is always strong from 145m to 500m depth. This could be explained by the vertical structure of Kelvin waves in the Ombai Strait. Sprintall et al. (2009b) argued that in May 2004, a downwelling Kelvin wave dominated the strong flow reversal from surface to 700m in the Ombai Strait.

In addition to the semi-annual intra-seasonal frequency, there is a response at other intra-seasonal frequencies seen clearly at 140m depth. Two of the most notable are the third and fourth peak with a period of about 90 and 60 days. Iskandar et al. (2006) mentioned that the variation with a period of 90 days dominates the surface current. And the 60-day variations are the most prominent feature of the subsurface current. These are higher-frequency signals that could be driven by local wind and intrinsic flow variability and are out of the scope of this project.

3.2 Variability from OFAM3

Observation of the ITF variability from INSTANT indicated that there are Kelvin waves in the major outflow passages into the Indian Ocean. The time series and frequency spectra can now be compared with the results from ocean model simulations. Understanding how well Kelvin waves and corresponding intra-seasonal variability are simulated by global and regional high-resolution ocean models was the main focus of this project. In this section, variability from the OFAM3 model will be shown. In addition to time series, ocean models offer us an opportunity to look at spatial maps of anomalies and see the evolution and propagation of Kelvin waves. Below, we use horizontal maps of the ITF temperature anomaly at 145m depth to illustrate and describe the duration and amplitude of Kelvin waves approaching outflow passages from the Indian Ocean.

3.21 Temperature anomaly

According to the results from INSTANT described above, the seasonal cycle of the velocity is dominant at 300m depth in the Ombai Passage, while the intra-seasonal velocity variability is dominant at 145m depth. Hence, we chose 145m depth where intra-seasonal variabilities were shown to clearly illustrate Kelvin waves in the model, which is very close to the 140m depth used in the analysis of INSTANT observations above.

The evolution of a positive temperature anomaly at 145m depth associated with the eastward propagation of a Kelvin wave is shown in Fig. 11. The time series of temperature anomalies versus depth from INSTANT is also shown below because it allows us to connect the observed temperature anomalies and their vertical distribution with the propagating Kelvin waves shown in horizontal maps. Fig.12 shows how temperature variability is captured in three straits (Ombai, Lombok and Timor) in the OFAM3 model. It also shows the variability of the ITF from the 2004 to 2006 time period is similar to that observed during the INSTANT program.

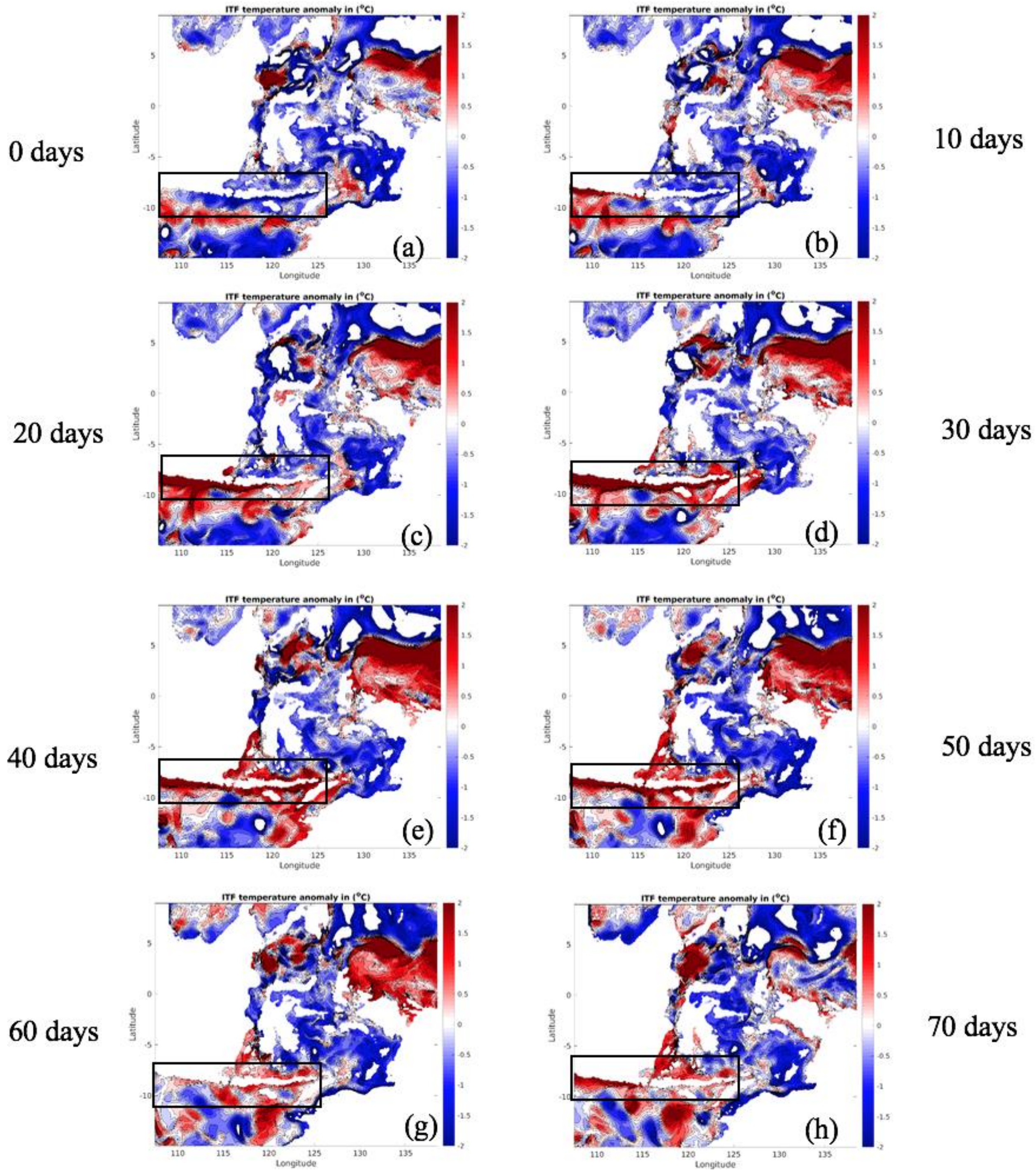

Figure 11 | Eastward propagation of a Kelvin wave illustrated by a positive temperature anomaly from OFAM3 model. Units are ^{0}C

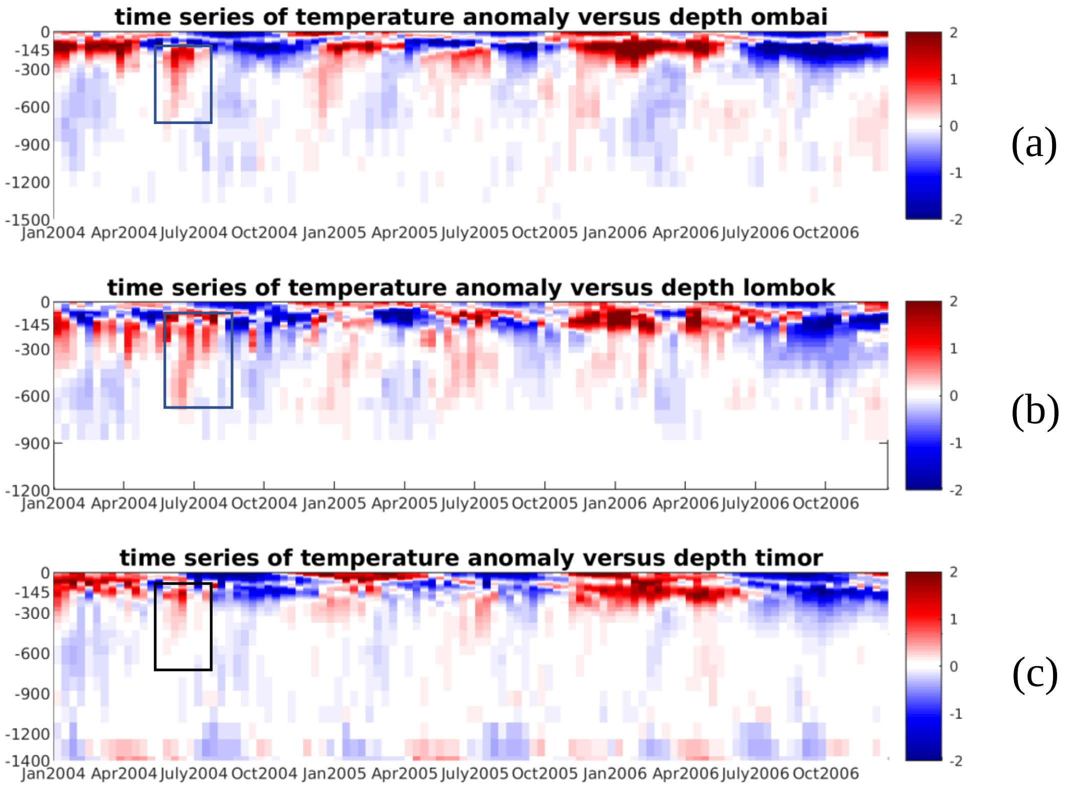

Figure 12 | Time series of temperature anomalies versus depth from OFAM3 model. Units are ^{0}C.

Fig.11a-h shows the evolution of a positive temperature anomaly from its appearance on the west side of the domain, followed by its propagation eastward towards Ombai, to its disappearance. We can estimate the duration of this disturbance representing a positive Kelvin wave of about 60 days.

Kelvin waves were captured by the time series of temperature anomaly versus depth in three straits. The propagation of the positive Kelvin wave between 0 and 60 days is highlighted in Fig.12a corresponding to a positive temperature anomaly from May to June of 2004. First, there was no positive anomaly (Fig.11a, 0 days). Then a weak positive temperature anomaly appeared near the Java, Lombok and Ombai islands (Fig.11b, 10 days). Then, a stronger anomaly appeared, meaning the Kelvin wave propagates eastward and reaches the coast of the Java sea (Fig.11c, 20 days). It reached the highest amplitude, filling up the Ombai strait and reaching the Timor Passage, at 30 days (Fig.11d). We can see some part of the positive temperature anomaly propagating northward through Lombok into the Makassar strait.

Meanwhile, most of the anomaly continued to propagate eastward, through Ombai and then around the islands into the Banda Sea. A small fraction of the anomaly propagated through the Timor Passage into the Indonesian Sea, where the colour is light blue on the horizontal maps. There was a decreasing trend of the anomaly at about 40-50 days (Fig.11e and Fig.11f). Finally, the Kelvin wave became very weak and disappeared (Fig.11g).

There was a similar, negative intra-seasonal event caused by the Kelvin wave which is not shown. Both positive and negative Kelvin waves had a duration of about 60 days. Though the amplitude of the negative Kelvin waves was smaller, both were linked to temperature anomalies in the time series versus depth. Maps of the anomaly evolution showed that most of the Kelvin waves propagated into the Indonesian sea through the Ombai strait, with some going northward through the Lombok strait and a small amount through the Timor strait.

Fig.12b and Fig.12c shows the time series of temperature anomaly versus depth in the Lombok and Timor straits. Compared to the anomaly in the Ombai strait, the distribution of the intra-seasonal variability was mainly consistent, though the amplitude was smaller. Most of them were concentrated at 145m depth and the period of the Kelvin waves was approximately 60 days.

3.22 Velocity anomaly

In addition to temperature anomaly, velocity anomaly is also thought to be a good indicator of the presence of Kelvin waves. Therefore, we’ve also shown the horizontal maps of the velocity anomaly at 145m depth and its time series produced by the OFAM3 model. The positive phase of an intra-seasonal oscillation of velocity anomalies at 145m depth representing a Kelvin wave is shown in Fig.13. As before, we chose three different straits to observe the Kelvin wave. Time series of velocity anomalies versus depth are shown in Fig.14, for the same period: from 2004 to 2006.

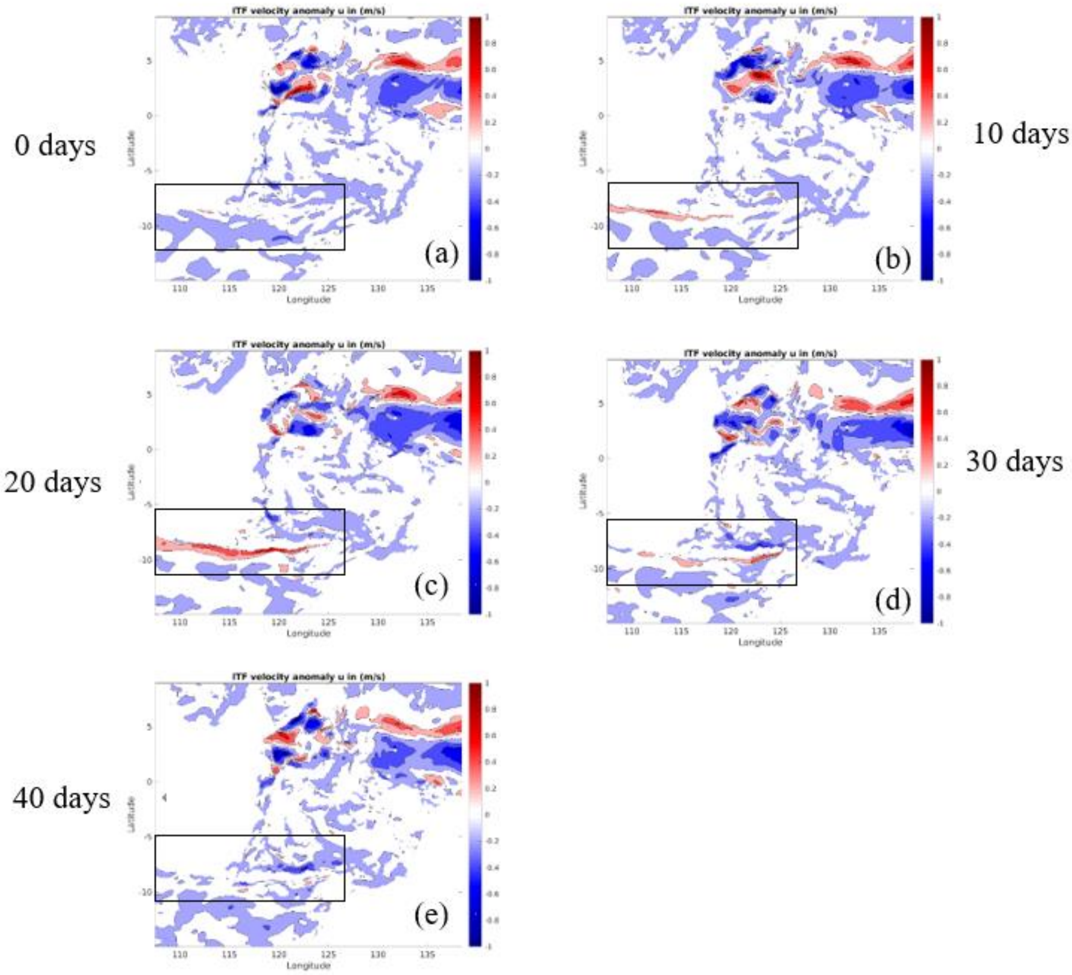

Figure 13 | Eastward propagation of a Kelvin wave illustrated by a positive velocity anomaly from OFAM3 model. Units are m/s

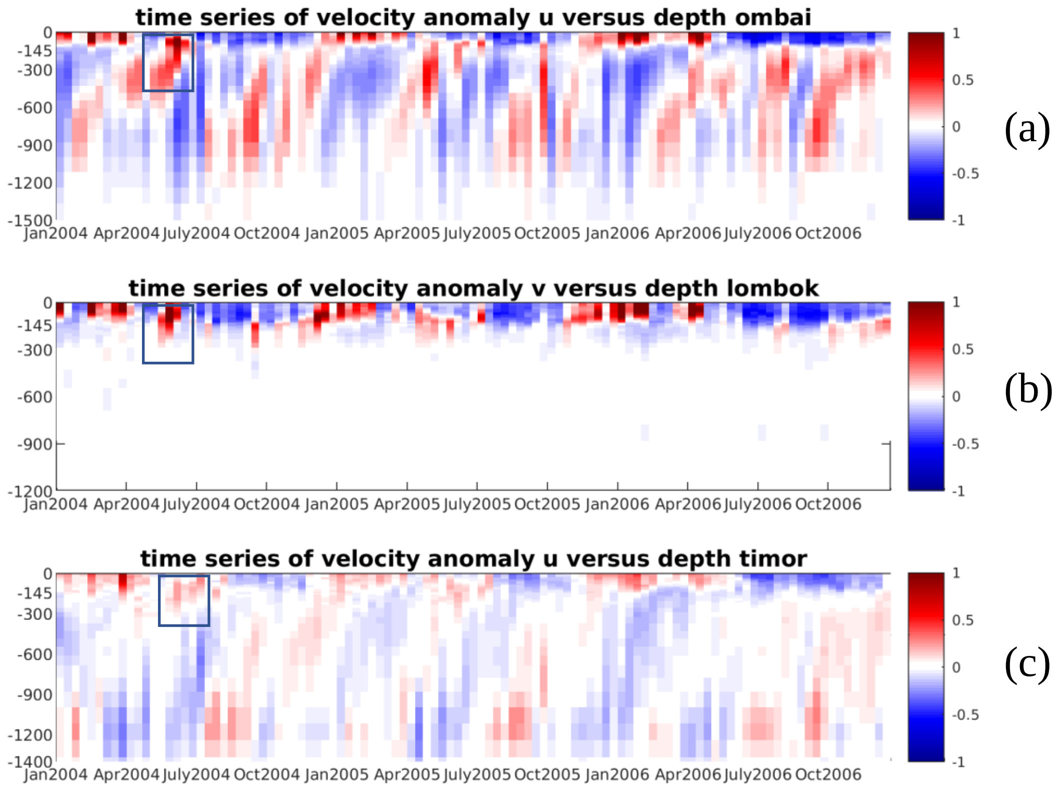

Figure 14 | Time series of velocity anomalies versus depth from OFAM3 model. Units are m/s.

It is worth mentioning that the coordinate system used for velocity in the model is different from that used for the INSTANT data. In the INSTANT program, an along and across strait coordinate system was used, which means the x-axis and y-axis are in the direction of the along and across strait velocity in each strait. However, the coordinate system used in the models is along the conventional zonal and meridional directions. The along strait velocity in the INSTANT data provides a good indicator to show the intra-seasonal variability of the flow that goes through the strait. In the horizonal anomaly maps from the model, we chose velocity anomaly component u to illustrate the Kelvin waves, because the Kelvin waves roughly propagate eastward along the island chain. However, for the time series of velocity anomaly versus depth in all three straits, the choice was different for each strait. Because the direction along the Lombok is mainly meridional while the Ombai and Timor are zonal, we choose velocity component v for Lombok and u for the Ombai and Timor Straits.

Fig.13 shows a complete evolution process for a positive Kelvin wave from appearance to disappearance in velocity anomaly signal. This evolution process occurred from May to June 2004 in Fig.13a-e and is also highlighted in Fig.14a. Similar to the temperature anomaly, the positive velocity anomaly began to appear with a small amplitude at 10 days (Fig.13b, 0.3 m/s). Then, the amplitude grew with the strongest anomaly occurring at 20 days and reaching 0.8 m/s (Fig.13c). In the next 20 days, the Kelvin wave became weaker, gradually and finally disappearing near the Ombai Strait (Fig.13d-e). A negative Kelvin wave has a similar behavior and is not shown.

The evolution of a Kelvin wave from its appearance in the model domain to its disappearance near the Ombai Strait had a duration of about 50 days. The wave appearance and disappearance were more clearly indicated by the velocity anomaly than temperature. This is likely because velocity better tracks the propagation of the waves, while the temperature anomaly might stay after the wave disappears. Fig.14b and Fig.14c shows the time series of the velocity anomaly in the Lombok and Timor straits, which are a little different from that in Ombai. Timor shows weaker variability from the surface to about 1400m, which is deeper than in the Ombai Strait. The variability of the Lombok Strait below 300m depth is so small that almost no signal was captured.

3.23 Kinetic energy frequency spectra

The horizontal maps of temperature and velocity anomaly can show how Kelvin waves come and go along the coast and their pathways before they enter into the strait. The horizontal maps give us information about the spatial distribution of waves. In this project, we sought to to quantify the variability driven by Kelvin waves and to compare this variability to observations. We estimated the kinetic energy spectra from the model and used the spectra to quantify the variability due to Kelvin waves in three major outflow passages. Then, below (3.4 Comparison between model and observation) we also compared spectra from the model to those estimated from observations in order to validate the model. Therefore, similar to the analysis done for INSTANT observations above, we estimated the frequency spectra for 3 straits at 145m depth using now by the OFAM3 model outputs.

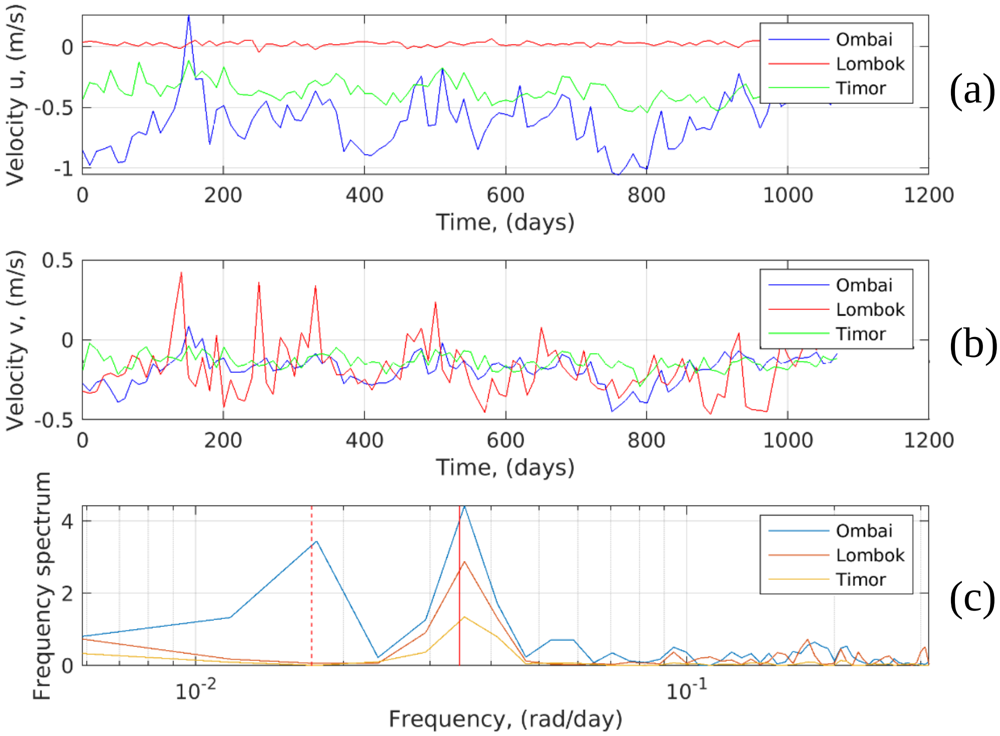

Figure 15 | (a) Time series of along velocity in Ombai and Timor and across velocity in Lombok at -145m depth;

(b) Time series of along velocity in Lombok and across velocity in Ombai and Timor at -145m depth;

© Frequency spectrum in Ombai, Lombok and Timor at -145m depth.

Red dash line: The frequency which represents the period of one year.

Red line: The frequency which represents the period of a half year.

In Fig.15, we can see strong seasonal cycle and semiannual variability signals that correspond to the first and second peaks in the figure. The semiannual variability represents the Kelvin waves. The energy of Kelvin waves, represented by the level of the spectrum at semiannual frequency, exceeds over that of the seasonal cycle. The flow in the Ombai and Timor Straits was dominated by the u component because of the mainly zonal direction. The v component was dominant in the Lombok strait (Fig.15b) where the flow is predominantly meridional. In order to keep consistency with the INSTANT program, the frequency spectra were also calculated by the total velocity, which includes the u and v component. Interestingly, there was no strong seasonal cycle in Lombok at 145m depth. A seasonal cycle was not found in the Timor Strait either. Sprintall et al. (2019a) provided an interpretation that although there is a weak subsurface maximum at 50 to 60m depth for the flow in the Lombok and Timor straits, the vertical transport distribution mainly showed a surface intensification. In addition to the surface maximum, there was also a similarly strong subsurface flow maximum at about 180m depth in Ombai. That is likely why only the Ombai strait showed a clear seasonal cycle at 145m depth, while the Lombok and Timor straits had a seasonal cycle pronounced near the surface. While Kelvin waves are present in all three straits, we can also see that the energy at semiannual frequency in Timor is about half of that in the Lombok Strait.

The amplitude of the spectrum was consistent with the time series and horizontal anomaly map figures. All these plots show that the anomalies and their variability were strongest the Ombai Strait and weakest in Timor. This suggests that Kelvin waves mainly propagate into Indonesian seas through the Ombai strait, with some portion of their energy propagating northward into the Lombok strait. A small amount of energy makes it to the Timor strait.

How the Kelvin waves were represented at different depths is essential for validating the model. Therefore, the frequency spectra at 300 and 500m depth are shown.

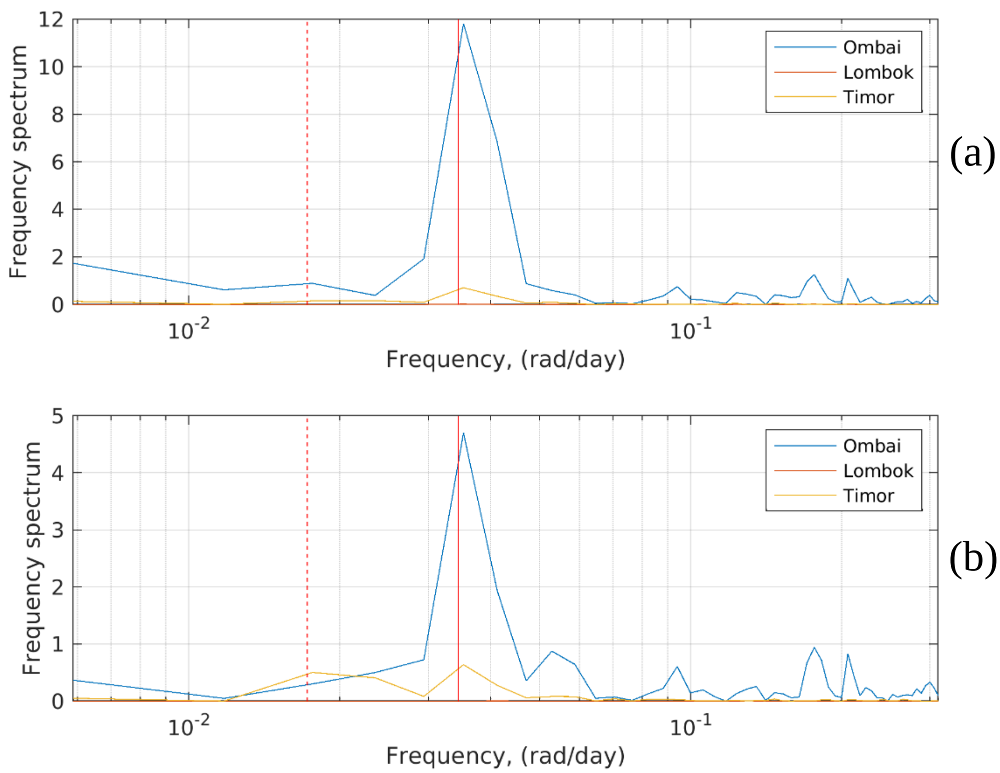

Figure 16 | (a) Frequency spectrum in Ombai, Lombok and Timor at -300m depth. b) Frequency spectrum in Ombai, Lombok and Timor at -500m depth.

Red dash line: The frequency which represents the period of one year.
Red line: The frequency which represents the period of a half year.

At the 300m and 500m depth, the seasonal cycles were both much weaker compared to the intra-seasonal variability caused by the Kelvin waves, proving again that the seasonal variability is dominant in the upper layer of the ocean. What we focussed on was the intra-seasonal variability which represents the Kelvin waves. In Fig.16a, there were extremely strong Kelvin waves in the Ombai Strait. The Kelvin wave in the Timor strait is much weaker and there was no intra-seasonal variability in the Lombok strait. However, the intra-seasonal variability was shown differently at 500m depth (Fig.16b). There was a clear Kelvin wave in the Ombai strait, but the energy was only about one third of that at 300m depth. The Kelvin wave in the Timor strait also became weaker, with half the energy at 500m compared to 300m depth. Again, intra-seasonal variability was not observed in the Lombok Strait. The different vertical distributions of Kelvin waves in the three Straits can be partly explained by the observations of Sprintall et al. (2009b). The intra-seasonal variability that represents Kelvin waves in the Ombai strait was found from 700m depth to surface. The Kelvin wave in Lombok dominated the depth above 300m, while the Kelvin wave was weaker between 300m to 0m in the Timor strait, and the variability was evident at subthermocline to intermediate depths.

In summary, the Kelvin waves in the Lombok and Timor straits were dominant at 145m depth, while the Kelvin waves in the Ombai Strait were evident from 500m to 145m, reaching a maximum at 300m depth. This is consistent with the analysis for the evolution and propagation of Kelvin waves at 145m depth only, because the total Kelvin waves was concentrated at the 145m depth for the Lombok and Timor Straits and the waves in Ombai is also dominant for three straits.

3.3 Variability from high-resolution regional model

In this section, I describe the intra-seasonal variability driven by Kelvin waves as simulated by the high-resolution regional model. As for OFAM3, the regional model allows us to study spatial maps of anomalies in addition to their time series in the outflow straits. The evolution and propagation of Kelvin waves, as well as their duration and amplitude, are demonstrated by the horizontal maps of the ITF temperature anomaly. Here, we also chose 145m depth which is same the depth we chose in the INSTANT and OFAM3 models.

3.31 Temperature anomaly

The evolution of a positive temperature anomaly at 145m depth associated with the eastward propagation of a Kelvin wave is shown in Fig. 17. The time series of temperature anomalies versus depth, as done in the INSTANT observations and OFAM3 model results, is also shown below in Fig. 18. Using a combination of anomaly maps and time series plots allowed us to connect the observed temperature anomalies and their vertical distribution with the propagation of Kelvin waves throughout the region. Fig. 18 shows the temperature variability in three outflow straits (Ombai, Lombok and Timor) in the regional model. It also shows the 3 year variability of the ITF. Three years is a similar duration to that chosen in the INSTANT program and OFAM3 model. An important thing, is that the regional model has no calendar because it is forced by a repeat year forcing from 1990-1991. Therefore, the times are shown as year1, year2 and year3 in time series plot in the regional model. (The same method is used in the section below when the time series of the regional model is mentioned.)

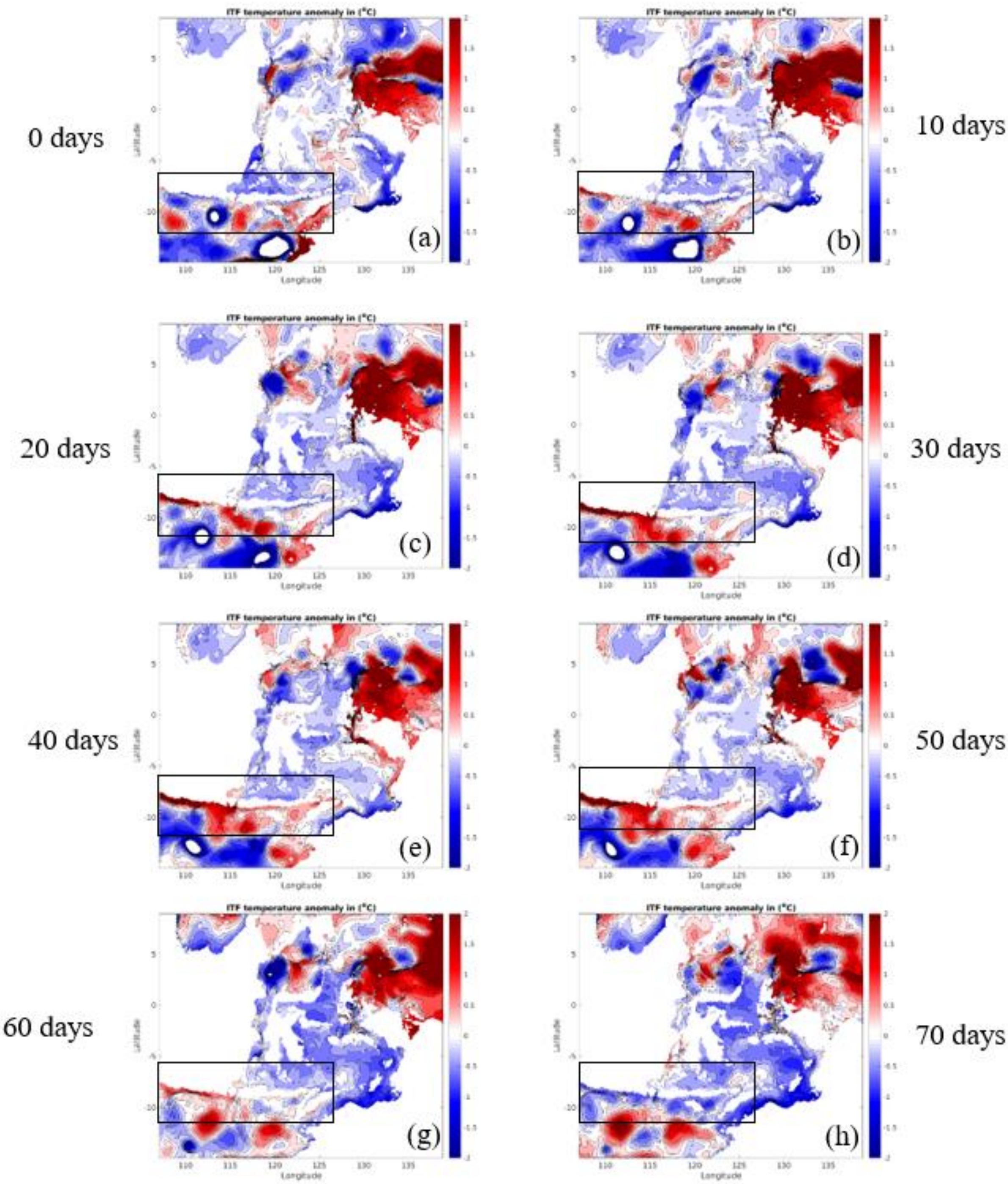

Figure 17 | Eastward propagation of a Kelvin wave illustrated by a positive temperature anomaly from the regional ITF model. Units are ^{0}C

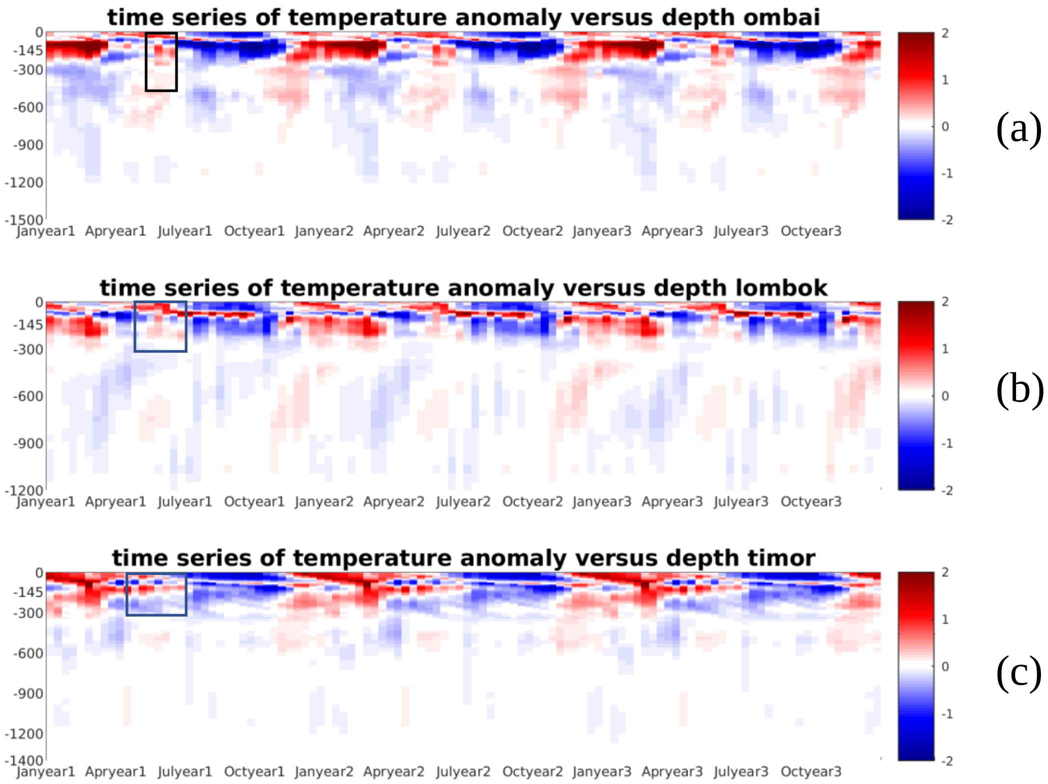

Figure 18 | Time series of temperature anomalies versus depth from the regional ITF model. Units are ^{0}C.

A complete evolution of a positive temperature anomaly from appearance to disappearance is shown in Fig.17a-h. Similar to the results from OFAM3, the duration of this disturbance representing a positive Kelvin wave was about 60 days. This Kelvin wave was also captured by the time series of temperature anomaly versus depth in three straits. The whole propagation of the positive Kelvin wave between 0 and 60 days is highlighted in Fig.18a corresponding to a positive temperature anomaly from May to June of year1.

The evolution of a positive Kelvin wave in the regional ITF model followed similar stages to those in the OFAM3 model described above. To begin with, there was no positive anomaly (Fig.17a, 0 days). Then a weak positive temperature anomaly appeared near the Java, Lombok and Ombai islands (Fig.17b, 10 days). There was an increasing trend of the anomaly at about 20-30 days and the Kelvin wave propagated eastward, reaching the coast of Java ((Fig.17c and d)). After that, it reached the highest amplitude, filled up the Ombai strait and reached the Timor Passage at 40-50 days (Fig.17e and f). Finally, the Kelvin wave became weak and disappeared. (Fig.17g and h, 60-70days). While we can see that some part of the positive temperature anomaly propagated northward into the Makassar strait through the Lombok strait, the magnitude of this signal was significantly smaller in the regional ITF model than in OFAM3. Also, some of the warm signal propagated eastward into the Banda sea through the Ombai strait and the Timor strait, but the magnitude of that warming in response to the Kelvin wave was, again, smaller in the regional ITF model than in OFAM3. Fig.18b and Fig.18c show the Kelvin wave signal clearly both in the Ombai and Lombok straits, however, in the Timor strait, the Kelvin wave is not evident, especially at depth.

In summary, the horizontal propagation and time series of temperature or velocity anomalies were qualitatively consistent between OFAM3 and the regional ITF model. However, the temperature anomalies in the three straits at 145m depth from the regional ITF model weren't as strong as those in OFAM3. In addition, there were no strong positive anomalies propagating into the Indonesian seas in the regional ITF model. It seems that the Kelvin waves disappear rapidly after approaching and passing through the three straits. The differences between the two models could be explained by the different forcing used to drive the two models. For instance, in the OFAM3 model, the forcing is realistic interannual forcing from 2004 to 2006, while the regional ITF model is forced by outputs from ACCESS-OM-0.1 forced by a repeat-year forcing of 1990-1991. Differences in model physics and ocean bathymetry leading to rapid wave dissipation in the regional ITF model, could also be a reason for the difference in wave propagation between the two models.

3.32 Kinetic energy frequency spectra

To evaluate the intra-seasonal variability quantitatively, we estimated the frequency spectra for 3 straits at 145m, 300m and 500m depth from the regional ITF model outputs, (similarly to the analysis done for the OFAM3 model above).

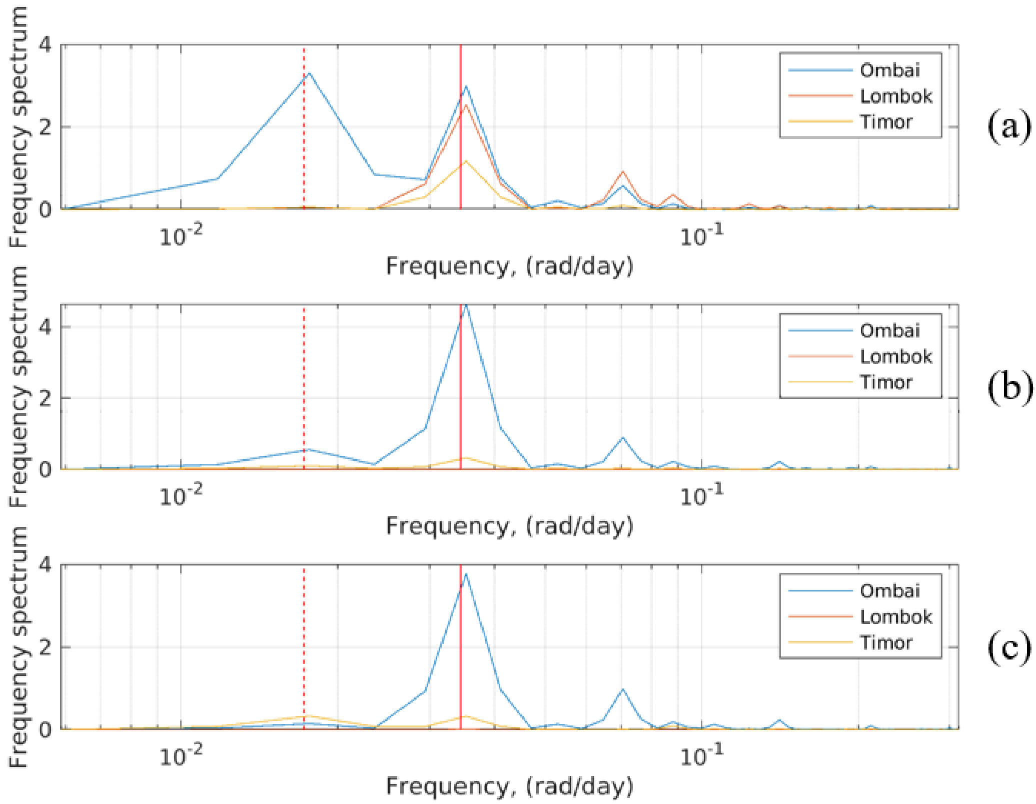

Figure 19 | (a) Frequency spectrum in Ombai, Lombok and Timor at -145m depth. (b) Frequency spectrum in Ombai, Lombok and Timor at -300m depth. (c) Frequency spectrum in Ombai, Lombok and Timor at -500m depth. Red dash line: The frequency which represents the period of one year. Red line: The frequency which represents the period of a half year.

In Fig.19a, a seasonal cycle, as indicated by the first peak, is clearly seen in the Ombai strait at 145m depth, while there is no strong seasonal variability signal in the Lombok and Timor straits. This result is consistent with the description of the seasonal variability based on observations in Sprintall et al. (2009b). The second peak of the frequency spectrum represents the 180-day period intra-seasonal variability driven by Kelvin waves. This variability is present in all three straits. The energy of the intra-seasonal variability in the Ombai and Lombok straits is nearly the same, with both being a factor of two stronger than in the Timor strait. This comparable contribution of Kelvin waves to the frequency spectrum in the three straits is consistent with similar light red color anomaly distributions shown in spatial maps. Given that the seasonal variability decays with depth, while the Kelvin wave-driven intra-seasonal remains evident, as in the analysis of OFAM3, we computed the frequency spectra at 300m and 500m depths (Fig.19b and c). The Kelvin waves showed similar properties at 300m and 500m depth in the three straits in the regional ITF model. At these two depths, Kelvin waves were clearly observed in the Ombai strait with almost the same amplitude, but were very weak in the Timor strait and cannot be observed very much at all in the Lombok strait.

The frequency spectra at 300m and 500m depth suggest that there are strong Kelvin waves only in the Ombai strait. Overall, if we focus on the depth levels from 500m to 145m, the Kelvin waves in the Ombai strait dominate the whole propagation of waves into the Indonesian seas. This implies that the Ombai strait is the main passage for Kelvin waves propagating eastward into the Indonesian seas. In addition, consistent with previous studies, our results also showed that some propagates energy into the Banda seas through the Timor strait and a small amount of energy propagates northward into Makassar strait through the Lombok strait.

3.4 Comparison between models and observation

To understand if the OFAM3 model and high-resolution regional ITF model represent the Kelvin waves and the associated intra-seasonal variability well, we compared the time series of temperature (velocity) anomaly versus depth and kinetic energy frequency spectra between INSTANT observations, OFAM3 and the regional ITF model.

3.41 Comparison of time series

We chose the time series of temperature and velocity anomaly from 2004 to 2006 in the Ombai strait below as an example to compare the observations from the INSTANT program and the model simulations.

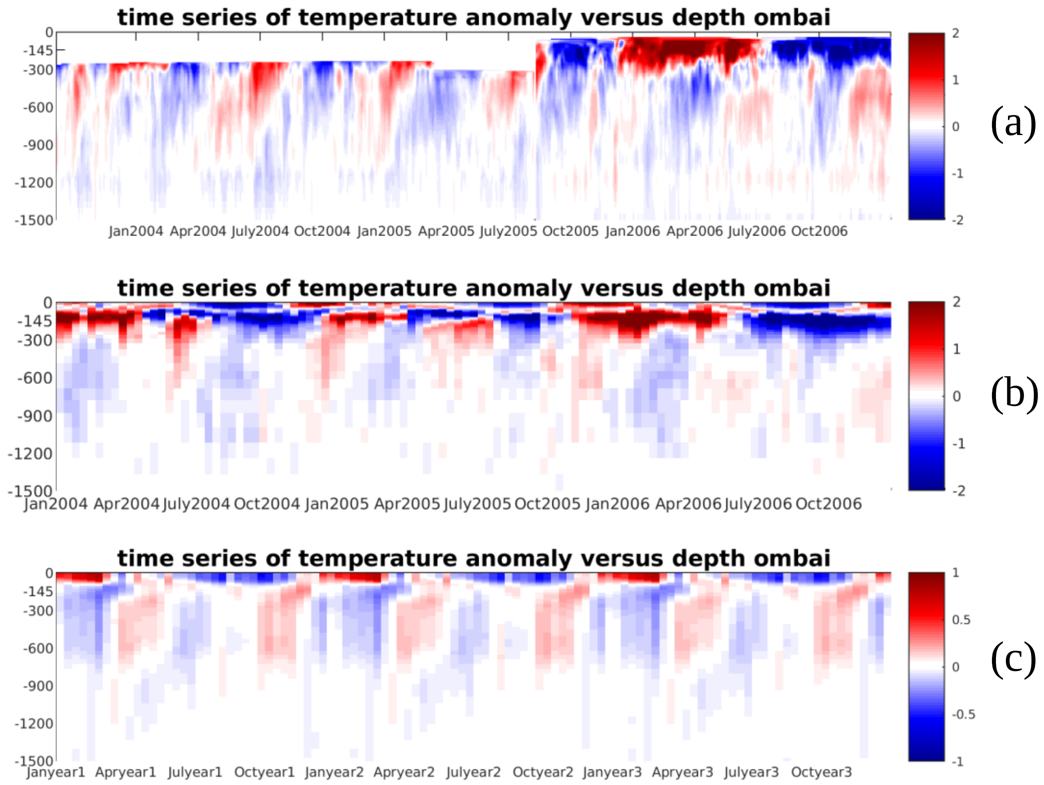

Figure 20 | Comparison of time series of temperature anomalies versus depth in Ombai strait between INSTANT program, OFAM3 model and regional ITF model. Units are ^{0}C.

(a) Time series from INSTANT program (The time series of Ombai strait in INSTANT has a duration more than 3 years, while only the 3 whole year time are labelled, which will be analysed).

(b) Time series from OFAM3 model.

(c) Time series from regional ITF model.

Because of a gap in the INSTANT data from 280m to the surface from 2005 to 2006 (Fig.20a), the seasonal cycle in the upper layers is not shown well. Comparing the time periods when INSTANT data are available, we can see that the OFAM3 and regional ITF model seem to represent the seasonal cycle well with the right frequency and anomaly amplitudes (Fig.20b and c). For the intra-seasonal variability, between 500m and 145m depth, the anomaly from OFAM3 and the regional ITF model are generally consistent with the anomaly from INSTANT.

Both OFAM3 and the regional ITF model can represent Kelvin waves well, though the Kelvin wave signal in the regional ITF model seems a little weaker than in OFAM3. For example, there is a clear positive anomaly from May to June which represents the downwelling Kelvin wave in Fig20a, b and c. In April 2006, an extremely strong variability occurred in the depth interval between 145m and 300m. However, in the regional ITF model, the variability is the same each year the model is driven by outputs from ACCESS-OM-0.1 forced by repeat-year-forcing from 1990-1991. In contrast, the simulations of the OFAM3 model forced by fully-realistic interannual forcing are more consistent with observations from the INSTANT program.

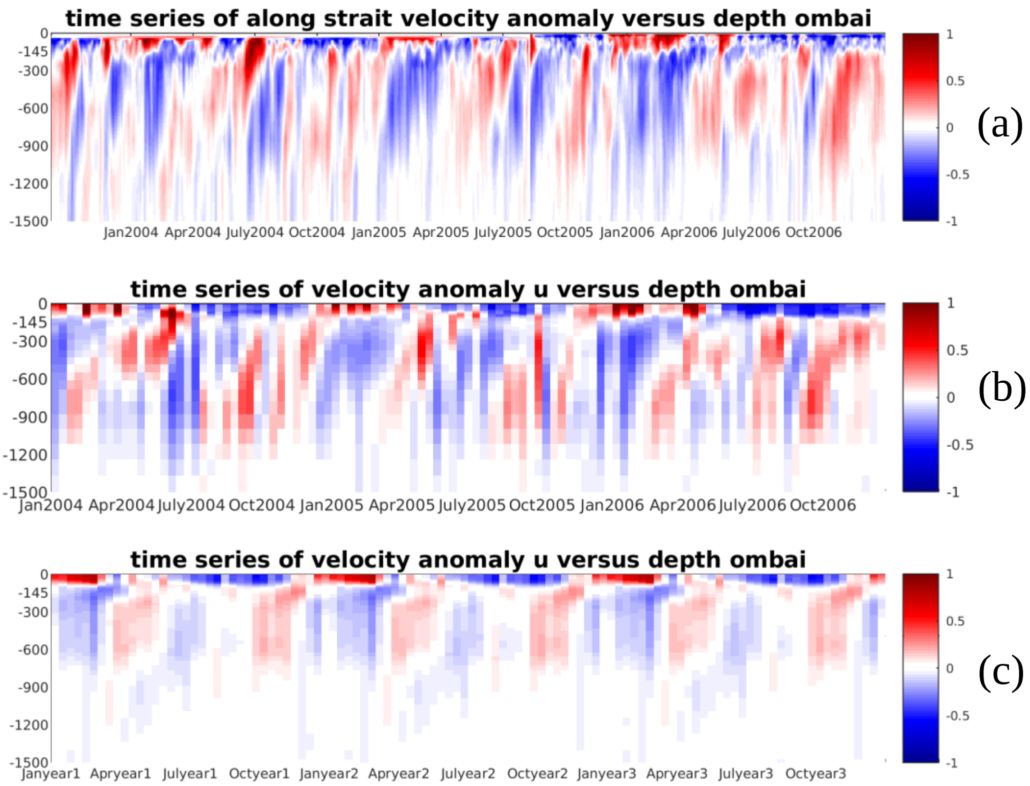

Figure 21 | Comparison of Time series of velocity anomalies versus depth between the INSTANT program, OFAM3 model and regional model. Units are m/s.

(a) Time series from the INSTANT program.

(b) Time series from the OFAM3 model.

(c) Time series from the regional model.

From the velocity time series in Fig. 21, the INSTANT and OFAM3 model results were quite consistent, while the regional ITF model tended to show less variability, particularly below 800m depth. That may be caused by the lower vertical resolution of the regional model at depth, as well as different forcing between the two models.

3.42 Comparison of kinetic energy frequency spectra

Finally, in addition to the time series of temperature and velocity anomalies, the frequency spectra can help to quantitatively describe the variability due to Kelvin waves in three major outflow passages. In this section, we choose the Ombai strait, which dominated the energy of Kelvin waves at 145m, 300m and 500m depth, and use it to make a comparison between the INSTANT, OFAM3 and regional ITF models.

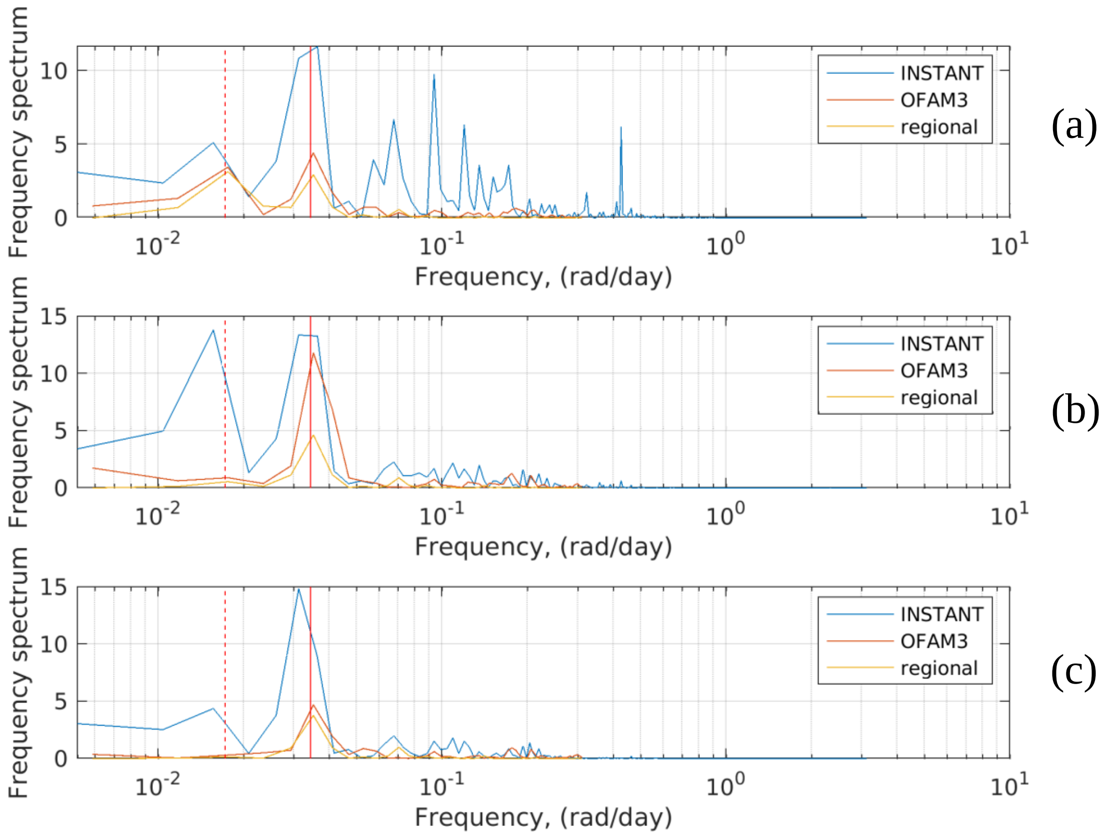

Figure 22 | (a) Comparison of frequency spectrum in Ombai strait at 145m depth between INSTANT data and OFAM3 and regional model.
(b) Comparison of frequency spectrum in Lombok strait at 300m depth between INSTANT data and OFAM3 and regional model.

(c) **Comparison of frequency spectrum in Timor strait at 500m depth between INSTANT data and OFAM3 and regional model.**

Red dash line: The frequency which represents the period of one year.

Red line: The frequency which represents period of half year.

In Fig.22a, the OFAM3 model and regional ITF model show a clear seasonal cycle with similar amplitude of the frequency spectrum. The energy of the seasonal cycle in the OFAM3 model and regional ITF model are much smaller than that in INSTANT. At 300m depth, only the observations from INSTANT show a clear seasonal cycle. The intra-seasonal variability driven by Kelvin waves also shows some differences between the observations and models. The Kelvin wave signal simulated by OFAM3 is comparable to that in observations at 300m depth, while the Kelvin waves in the regional model are weaker than in observations at all depths.

In summary, the output from the OFAM3 model was consistent with the INSTANT data for the time series figures that show the vertical distribution of seasonal and intra-seasonal variabilities. The regional model agrees qualitatively, but showed weaker anomalies and does not represent variability below 800m depth at all. As for the frequency spectrum, some differences in the energy of Kelvin waves cannot be neglected. Although OFAM3 and the regional ITF model simulated the seasonal cycle at 145m and even at the surface, the seasonal variability from 500m to 300m depths was not represented well. At 145m and 500m depths, both the OFAM3 model and regional ITF model produced a weaker Kelvin wave than in observations. The OFAM3 model simulated the Kelvin wave better at 300m depth. The horizontal maps of temperature and velocity showed qualitatively consistent Kelvin wave evolution, including wave duration, amplitude and propagation pathways.

4. Conclusion

The ITF shows strong variability on different time scales, including decadal, interannual, seasonal and intra-seasonal variability. The ITF variability on intra-seasonal time scales driven by remotely generated Kelvin waves that propagate into the Indonesian Seas from the Indian ocean has not been assessed in ocean models previously. In this project, we used the

OFAM3 model, a global ocean model, and a high-resolution regional model of the ITF to characterize these variabilities in three main outflow passages: the Ombai, Lombok and Timor Straits. In order to validate the ocean models, we also used available mooring observations from the INSTANT program.

The simulation from the OFAM3 model qualitatively agreed with that from the regional ITF model and with observations from the INSTANT program. The horizontal maps at 145m depth from these two models both showed a complete evolution of a positive temperature anomaly associated with the eastward propagation of a Kelvin wave. Our results suggest that the majority of Kelvin waves propagate into the Indonesian sea through the Ombai strait, with some going northward through the Lombok strait and a small number going through the Timor strait. The time series of temperature anomalies versus depth from the models were also consistent with observations showing seasonal cycle and intra-seasonal variabilities representing Kelvin waves from 800m depth to the surface. The frequency spectra from the models also demonstrated clear Kelvin wave signals at 145m, 300m and 500m depths consistent with observations.

However, quantitatively, there were still some differences between the two models and observations. The amplitude of the temperature anomaly corresponding to the Kelvin wave simulated by the regional model was weaker than in OFAM3. As the main passage that the Kelvin wave passed through into the Indonesian seas, the Ombai strait showed nearly the same energy of Kelvin waves at semiannual frequency for both the OFAM3 model and regional ITF model at 145m and 500m. However, the energy of Kelvin waves from observations was much greater, about twice as much as in the models. As for the 300m depth, the output from the OFAM3 model was similar to the observations, while the simulation from the regional ITF model was weaker. In addition, both models simulated quite weak higher-frequency variability, such as the 90-day-period and 60-day-period variabilities.

The time series of temperature or velocity anomalies imply that the regional ITF model does not capture the variability below 800m depth well. Also, there were almost no temperature anomalies propagating into the Indonesian seas in the regional ITF model, suggesting that either, weaker Kelvin waves are generated due to different forcing in that model, or that waves dissipate efficiently as they approach and propagate upstream through the outflow passages.

This study had a few limitations. Firstly, we have not compared variability in the same years for all models. The INSTANT observations were collected from 2004 to 2006. In the OFAM3 model we also analyzed years 2004-2006, however in the regional ITF model, we analyzed repeat-year forcing simulations corresponding to 1990-1991. The outputs simulated from different years may cause some differences in the intra-seasonal variability because the forcing may be different for each year. Secondly, the OFAM3 and ACCESS-OM-0.1 models used different parameters and parameterizations and hence the differences may also be due to different model physics. We haven't explored this. Finally, for the spectra calculations, the time period used was only 3 years. Ideally, we would analyze a longer time period.

In addition to resolving these limitations, there are other questions that can be addressed in the future. We intend to analyze high-resolution regional runs to study the role of resolution of the propagation and dissipation of Kelvin waves in the Indonesian Seas. Moreover, the analysis and comparison of interannual and repeat-year forcing runs in ACCESS-OM-0.1 could help to understand the physics of Kelvin waves. We plan to analyze different forcing in the same model to see the difference due to forcing, rather than model physics.

Reference

ADCROFT, A., HILL, C. & MARSHALL, J. 1997. Representation of Topography by Shaved Cells in a Height Coordinate Ocean Model. *Monthly Weather Review,* 125**,** 2293-2315.

ALORY, G., WIJFFELS, S. & MEYERS, G. 2007. Observed temperature trends in the Indian Ocean over 1960–1999 and associated mechanisms. *Geophysical Research Letters,* 34.

DEE, D. P. & UPPALA, S. 2009. Variational bias correction of satellite radiance data in the ERA-Interim reanalysis. *Quarterly Journal of the Royal Meteorological Society,* 135**,** 1830-1841.

FANG, G., SUSANTO, R. D., WIRASANTOSA, S., QIAO, F., SUPANGAT, A., FAN, B., WEI, Z., SULISTIYO, B. & LI, S. 2010. Volume, heat, and freshwater transports from the South China Sea to Indonesian seas in the boreal winter of 2007–2008. *Journal of Geophysical Research: Oceans,* 115.

FFIELD, A. & GORDON, A. L. 1992. Vertical Mixing in the Indonesian Thermocline. *Journal of Physical Oceanography,* 22**,** 184-195.

GODFREY, J. S. 1996. The effect of the Indonesian throughflow on ocean circulation and heat exchange with the atmosphere: A review. *Journal of Geophysical Research: Oceans,* 101**,** 12217-12237.

GORDON, A. L. 1986. Interocean exchange of thermocline water. *Journal of Geophysical Research: Oceans,* 91**,** 5037-5046.

GORDON, A. L., HUBER, B. A., METZGER, E. J., SUSANTO, R. D., HURLBURT, H. E. & ADI, T. R. 2012. South China Sea throughflow impact on the Indonesian throughflow. *Geophysical Research Letters,* 39.

GORDON, A. L., MA, S., OLSON, D. B., HACKER, P., FFIELD, A., TALLEY, L. D., WILSON, D. & BARINGER, M. 1997. Advection and diffusion of Indonesian Throughflow Water within the Indian Ocean South Equatorial Current. *Geophysical Research Letters,* 24**,** 2573-2576.

GORDON, A. L., SUSANTO, R. D., FFIELD, A., HUBER, B. A., PRANOWO, W. & WIRASANTOSA, S. 2008. Makassar Strait throughflow, 2004 to 2006. *Geophysical Research Letters,* 35.

GORDON, A. L., SUSANTO, R. D. & VRANES, K. 2003. Cool Indonesian throughflow as a consequence of restricted surface layer flow. *Nature,* 425**,** 824-828.

GRIFFIES, S. M. 2009. Elements of MOM4p1, GFDL Ocean Group Technical Report 6. *NOAA/Geophysical Fluid Dynamics Laboratory*.

HAUTALA, S. L., SPRINTALL, J., POTEMRA, J. T., CHONG, J. C., PANDOE, W., BRAY, N. & ILAHUDE, A. G. 2001. Velocity structure and transport of the Indonesian Throughflow in the major straits restricting flow into the Indian Ocean. *Journal of Geophysical Research: Oceans,* 106**,** 19527-19546.

HU, S. & SPRINTALL, J. 2016. Interannual variability of the Indonesian Throughflow: The salinity effect. *Journal of Geophysical Research: Oceans,* 121**,** 2596-2615.

ISKANDAR, I., TOZUKA, T., SASAKI, H., MASUMOTO, Y. & YAMAGATA, T. 2006. Intraseasonal variations of surface and subsurface currents off Java as simulated in a high-resolution ocean general circulation model. *Journal of Geophysical Research: Oceans,* 111.

KELLY, S. M., JONES, N. L., IVEY, G. N. & LOWE, R. J. 2015. Internal-Tide Spectroscopy and Prediction in the Timor Sea. *Journal of Physical Oceanography,* 45**,** 64-83.

KIDA, S. & WIJFFELS, S. 2012. The impact of the Indonesian Throughflow and tidal mixing on the summertime sea surface temperature in the western Indonesian Seas. *Journal of Geophysical Research: Oceans,* 117.

KISS, A. E., HOGG, A. M., HANNAH, N., BOEIRA DIAS, F., BRASSINGTON, G. B., CHAMBERLAIN, M. A., CHAPMAN, C., DOBROHOTOFF, P., DOMINGUES, C. M., DURAN, E. R., ENGLAND, M. H., FIEDLER, R., GRIFFIES, S. M., HEERDEGEN, A., HEIL, P., HOLMES, R. M., KLOCKER, A., MARSLAND, S. J., MORRISON, A. K., MUNROE, J., OKE, P. R., NIKURASHIN, M., PILO, G. S., RICHET, O., SAVITA, A., SPENCE, P., STEWART, K. D., WARD, M. L., WU, F. & ZHANG, X. 2019. ACCESS-OM2: A Global Ocean-Sea Ice Model at Three Resolutions. *Geosci. Model Dev. Discuss.,* 2019**,** 1-58.

KOCH-LARROUY, A., LENGAIGNE, M., TERRAY, P., MADEC, G. & MASSON, S. 2010. Tidal mixing in the Indonesian Sea and its effect on the tropical climate system. *Climate Dynamics,* 34.

KOCH-LARROUY, A., MADEC, G., BOURUET-AUBERTOT, P., GERKEMA, T., BESSIèRES, L. & MOLCARD, R. 2007. On the transformation of Pacific Water into Indonesian Throughflow Water by internal tidal mixing. *Geophysical Research Letters,* 34.

LEE, T., FUKUMORI, I., MENEMENLIS, D., XING, Z. & FU, L.-L. 2002. Effects of the Indonesian Throughflow on the Pacific and Indian Oceans. *Journal of Physical Oceanography,* 32**,** 1404-1429.

MARSHALL, J., ADCROFT, A., HILL, C., PERELMAN, L. & HEISEY, C. 1997. A finite-volume, incompressible Navier Stokes model for studies of the ocean on parallel computers. *Journal of Geophysical Research: Oceans,* 102**,** 5753-5766.

MASUMOTO, Y. & YAMAGATA, T. 1993. Simulated seasonal circulation in the Indonesian Seas. *Journal of Geophysical Research: Oceans,* 98**,** 12501-12509.

MASUMOTO, Y. & YAMAGATA, T. 1996. Seasonal variations of the Indonesian throughflow in a general ocean circulation model. *Journal of Geophysical Research: Oceans,* 101**,** 12287-12293.

MEYERS, G. 1996. Variation of Indonesian throughflow and the El Niño-Southern Oscillation. *Journal of Geophysical Research: Oceans,* 101**,** 12255-12263.

MOLCARD, R., FIEUX, M. & ILAHUDE, A. G. 1996. The Indo-Pacific throughflow in the Timor Passage. *Journal of Geophysical Research: Oceans,* 101**,** 12411-12420.

O. RICHET, M. N., B. PE˜NA-MOLINO, B. M. SLOYAN AND S. WIJFFELS 2019. The role of the seasonal variability on the background state of the Indonesian Seas. *JGR: Oceans*.

OKE, P. R., GRIFFIN, D. A., SCHILLER, A., MATEAR, R. J., FIEDLER, R., MANSBRIDGE, J., LENTON, A., CAHILL, M., CHAMBERLAIN, M. A. & RIDGWAY, K. 2013. Evaluation of a near-global eddy-resolving ocean model. *Geosci. Model Dev.,* 6**,** 591-615.

P.H. LEBLOND, L. A. M. 1978. Waves in the Ocean. Elsevier, Amsterdam, Elsevier Oceanography Series**,** 602.

PARIWONO, J. I., BYE, J. A. T. & LENNON, G. W. 1986. Long-period variations of sea-level in Australasia. *Geophysical Journal International,* 87**,** 43-54.

POTEMRA, J. T. 2001. Contribution of equatorial Pacific winds to southern tropical Indian Ocean Rossby waves. *Journal of Geophysical Research: Oceans,* 106**,** 2407-2422.

QIU, B., MAO, M. & KASHINO, Y. 1999. Intraseasonal Variability in the Indo–Pacific Throughflow and the Regions Surrounding the Indonesian Seas. *Journal of Physical Oceanography,* 29**,** 1599-1618.

SCHWARZKOPF, F. U. & BöNING, C. W. 2011. Contribution of Pacific wind stress to multi-decadal variations in upper-ocean heat content and sea level in the tropical south Indian Ocean. *Geophysical Research Letters,* 38.

SONG, Q. & GORDON, A. L. 2004. Significance of the vertical profile of the Indonesian Throughflow transport to the Indian Ocean. *Geophysical Research Letters,* 31.

SPRINTALL, J., GORDON, A. L., KOCH-LARROUY, A., LEE, T., POTEMRA, J. T., PUJIANA, K. & WIJFFELS, S. E. 2014a. The Indonesian seas and their role in the coupled ocean–climate system. *Nature Geoscience,* 7**,** 487.

SPRINTALL, J., GORDON, A. L., KOCH-LARROUY, A., LEE, T., POTEMRA, J. T., PUJIANA, K. & WIJFFELS, S. E. 2014b. The Indonesian seas and their role in the coupled ocean–climate system. *Nature Geoscience,* 7**,** 487-492.

SPRINTALL, J., GORDON, A. L., MURTUGUDDE, R. & SUSANTO, R. D. 2000. A semiannual Indian Ocean forced Kelvin wave observed in the Indonesian seas in May 1997. *Journal of Geophysical Research: Oceans,* 105**,** 17217-17230.

SPRINTALL, J., GORDON, A. L., WIJFFELS, S. E., FENG, M., HU, S., KOCH-LARROUY, A., PHILLIPS, H., NUGROHO, D., NAPITU, A., PUJIANA, K., SUSANTO, R. D., SLOYAN, B., PEñA-MOLINO, B., YUAN, D., RIAMA, N. F., SISWANTO, S., KUSWARDANI, A., ARIFIN, Z., WAHYUDI, A. A. J., ZHOU, H., NAGAI, T., ANSONG, J. K., BOURDALLE-BADIé, R., CHANUT, J., LYARD, F., ARBIC, B. K., RAMDHANI, A. & SETIAWAN, A. 2019a. Detecting Change in the Indonesian Seas. *Frontiers in Marine Science,* 6.

SPRINTALL, J., GORDON, A. L., WIJFFELS, S. E., FENG, M., HU, S., KOCH-LARROUY, A., PHILLIPS, H., NUGROHO, D., NAPITU, A., PUJIANA, K., SUSANTO, R. D., SLOYAN, B., YUAN, D., RIAMA, N. F., SISWANTO, S., KUSWARDANI, A., ARIFIN, Z., WAHYUDI, A. A. J., ZHOU, H., NAGAI, T., ANSONG, J. K., BOURDALLE-BADIé, R., CHANUT, J., LYARD, F., ARBIC, B. K., RAMDHANI, A. & SETIAWAN, A. 2019b. Detecting Change in the Indonesian Seas. *Frontiers in Marine Science,* 6.

SPRINTALL, J. & RéVELARD, A. 2014. The Indonesian Throughflow response to Indo-Pacific climate variability. *Journal of Geophysical Research: Oceans,* 119**,** 1161-1175.

SPRINTALL, J., WIJFFELS, S., GORDON, A. L., FFIELD, A., MOLCARD, R., SUSANTO, R. D., SOESILO, I., SOPAHELUWAKAN, J., SURACHMAN, Y. & VAN AKEN, H. M. 2004. INSTANT: A new international array to measure the Indonesian Throughflow. *Eos, Transactions American Geophysical Union,* 85**,** 369-376.

SPRINTALL, J., WIJFFELS, S. E., MOLCARD, R. & JAYA, I. 2009a. Direct estimates of the indonesian throughflow entering the indian ocean: 2004-2006. *Journal of Geophysical Research: Oceans,* 114.

SPRINTALL, J., WIJFFELS, S. E., MOLCARD, R. & JAYA, I. 2009b. Direct estimates of the Indonesian Throughflow entering the Indian Ocean: 2004–2006. *Journal of Geophysical Research: Oceans,* 114.

SUSANTO, R. D. & GORDON, A. L. 2005. Velocity and transport of the Makassar Strait throughflow. *Journal of Geophysical Research: Oceans,* 110.

TSUJINO, H., URAKAWA, S., NAKANO, H., SMALL, R. J., KIM, W. M., YEAGER, S. G., DANABASOGLU, G., SUZUKI, T., BAMBER, J. L., BENTSEN, M., BöNING, C. W., BOZEC, A., CHASSIGNET, E. P., CURCHITSER, E., BOEIRA DIAS, F., DURACK, P. J., GRIFFIES, S. M., HARADA, Y., ILICAK, M., JOSEY, S. A., KOBAYASHI, C., KOBAYASHI, S., KOMURO, Y., LARGE, W. G., LE SOMMER, J., MARSLAND, S. J., MASINA, S., SCHEINERT, M., TOMITA, H., VALDIVIESO, M. & YAMAZAKI, D. 2018. JRA-55 based surface dataset for driving ocean–sea-ice models (JRA55-do). *Ocean Modelling,* 130**,** 79-139.

VECCHI, G. A., SODEN, B. J., WITTENBERG, A. T., HELD, I. M., LEETMAA, A. & HARRISON, M. J. 2006. Weakening of tropical Pacific atmospheric circulation due to anthropogenic forcing. *Nature,* 441**,** 73-76.

VRANES, K., GORDON, A. L. & FFIELD, A. 2002. The heat transport of the Indonesian Throughflow and implications for the Indian Ocean heat budget. *Deep Sea Research Part II: Topical Studies in Oceanography,* 49**,** 1391-1410.
WAINWRIGHT, L., MEYERS, G., WIJFFELS, S. & PIGOT, L. 2008. Change in the Indonesian Throughflow with the climatic shift of 1976/77. *Geophysical Research Letters,* 35.
WEI, J., LI, M. T., MALANOTTE-RIZZOLI, P., GORDON, A. L. & WANG, D. X. 2016. Opposite Variability of Indonesian Throughflow and South China Sea Throughflow in the Sulawesi Sea. *Journal of Physical Oceanography,* 46**,** 3165-3180.
WHITEWAY, T. G. 2009. Australian Bathymetry and Topography Grid. *Geoscience Australia Record,* 21**,** 46.
WIJFFELS, S. & MEYERS, G. 2004. An Intersection of Oceanic Waveguides: Variability in the Indonesian Throughflow Region. *Journal of Physical Oceanography,* 34**,** 1232-1253.
WIJFFELS, S. E., MEYERS, G. & GODFREY, J. S. 2008. A 20-Yr Average of the Indonesian Throughflow: Regional Currents and the Interbasin Exchange. *Journal of Physical Oceanography,* 38**,** 1965-1978.
WYRTKI, K. 1961. Physical Oceanography of the Southeast Asian waters. *Scripps institution of oceanography*.
WYRTKI, K. 1973. An Equatorial Jet in the Indian Ocean. *Science,* 181**,** 262-264.
.